The Journal of Neuroscience, September 15, 1998, *18*(18):7216–7231

Altered Ca^{2+} Signaling and Mitochondrial Deficiencies in Hippocampal Neurons of Trisomy 16 Mice: A Model of Down's Syndrome

Sebastian Schuchmann, Wolfgang Müller, and Uwe Heinemann

Department of Neurophysiology, Institute of Physiology, Charité, Humboldt University Berlin, D-10117 Berlin, Germany

It has been suggested that augmented nerve cell death in neurodegenerative diseases might result from an impairment of mitochondrial function. To test this hypothesis, we investigated age-dependent changes in neuronal survival and glutamate effects on Ca^{2+} homeostasis and mitochondrial energy metabolism in cultured hippocampal neurons from diploid and trisomy 16 (Ts16) mice, a model of Down's syndrome. Microfluorometric techniques were used to measure survival rate, $[Ca^{2+}]_i$ level, mitochondrial membrane potential, and NAD(P)H autofluorescence. We found that Ts16 neurons die more than twice as fast as diploid neurons under otherwise identical culture conditions. Basal $[Ca^{2+}]_i$ levels were elevated in Ts16 neurons. Moreover, in comparison to diploid neurons, Ts16 neurons showed a prolonged recovery of $[Ca^{2+}]_i$ and mitochondrial membrane potential after brief glutamate application. Glutamate evoked an initial NAD(P)H decrease that was found to be extended in Ts16 neurons in comparison to diploid neurons. Furthermore, for all age groups tested, glutamate failed to cause a subsequent NAD(P)H overshoot in Ts16 cultures in contrast to diploid cultures. In the presence of cyclosporin A, an inhibitor of the mitochondrial membrane permeability transition, NAD(P)H increase was observed in both diploid and Ts16 neurons. The results support the hypothesis that Ca^{2+} impairs mitochondrial energy metabolism and may play a role in the pathogenesis of neurodegenerative changes in neurons from Ts16 mice.

Key words: trisomy 16; Down's syndrome; Alzheimer's disease; hippocampal culture; calcium; mitochondrial membrane potential; NAD(P)H

The presence of an extra copy of human chromosome 21 [trisomy 21 (Ts21)] leads to the genesis of Down's syndrome, a disorder associated with mental retardation, facial dysmorphology, and congenital heart disease. Individuals with Down's syndrome are known to have a tendency to develop neuropathological features of Alzheimer's disease in the third decade of life. This observation has led to the suggestion that the overexpression of gene products from chromosome 21 is responsible for the early onset of Alzheimer's disease (Richards et al., 1991). Indeed, plaques containing β-amyloid protein (βAP) have been found in the brain of Ts21 individuals (Rumble et al., 1989), presumably as a result of overexpression of the β-amyloid precursor protein (βAPP), which is encoded on chromosome 21.

The trisomy 16 mouse (Ts16) is a model of Down's syndrome (Ts21) and to some extent also of Alzheimer's disease (Coyle et al., 1988; Colton et al., 1990). At least nine genes mapped on human chromosome 21 are also located on mouse chromosome 16, including the genes for superoxide dismutase (SOD) and βAPP (Richards et al., 1991; Holtzman et al., 1992). As with individuals with Down's syndrome, Ts16 fetal mice exhibit edema of the neck, inner ear anomalies, congenital heart disease, and retardation in CNS development (for review, see Epstein, 1986). The Ts16 mouse model is limited, however, by the fact that Ts16 fetuses usually die at gestation day 18–20 (Richards, 1991) because of Ts16-induced disturbances in the cardiovascular system. To overcome the limitation presented by death *in utero* and to increase neuronal survival times, we used dissociated hippocampal cell cultures for our studies.

Previous studies suggested that cultured neurons from Ts16 mice show altered electrogenesis possibly associated with augmented Ca^{2+} loading of cells (Orozco et al., 1988; Ault et al., 1989; Galdzicki et al., 1993). In such cultures, neuronal cell loss has been shown to be accelerated (Stabel-Burow et al., 1997). Furthermore, cultured hippocampal Ts16 mice neurons display an inherited defect in survival response mediated by glutamate in low concentration (Bambrick et al., 1995). Among the overexpressed proteins in this model is βAPP, which has been shown to have a role in the regulation of intracellular Ca^{2+} (Mattson et al., 1993b). In contrast, the βAPP product βAP, which had been demonstrated to occur in Ts16 hippocampal neurons (Richards et al., 1991), is suspected to destabilize intracellular calcium homeostasis and render neurons more vulnerable to excitotoxicity (Mattson et al., 1992).

Disturbed Ca^{2+} homeostasis may lead to neuronal cell loss by various mechanisms (Choi, 1995; Mattson et al., 1995). One of the possibilities is that increased $[Ca^{2+}]_i$ causes depolarization of mitochondrial membrane and thereby disturbs the respiratory chain and the subsequent production of ATP (Aw et al., 1987; Richter and Kass, 1991; Duchen and Biscoe, 1992). Reduced ATP supply will ultimately interfere with electrolyte homeostasis and the transport processes of cellular substrates. Furthermore, a dysfunction of the mitochondrial electron transport chain will lead to a disturbance in the $NAD(P)^+$/NAD(P)H ratio (Hansford, 1980). The associated shift in the mitochondrial redox bal-

Received April 30, 1998; revised June 23, 1998; accepted June 26, 1998.

This study was supported by the Graduiertenkolleg "Schadensmechanismen im zentralen Nervensystem (ZNS): Einsatz bildgebender Verfahren" and the Sonderforschungsbereich (SFB) 507 TP C4. We thank Dr. H. Winking for kindly supplying the trisomy 16 mice. We gratefully acknowledge technical support from Dr. H. Siegmund, Dr. H. J. Gabriel, S. Latta, and A. Düerkop. Many thanks to Dr. D. Bilkey, R. Kemp, and Dr. D. Schmitz for critical reading of this manuscript.

Correspondence should be addressed to S. Schuchmann, Department of Neurophysiology, Institute of Physiology, Charité, Humboldt University Berlin, Tucholskystrasse 2, D-10117 Berlin, Germany.

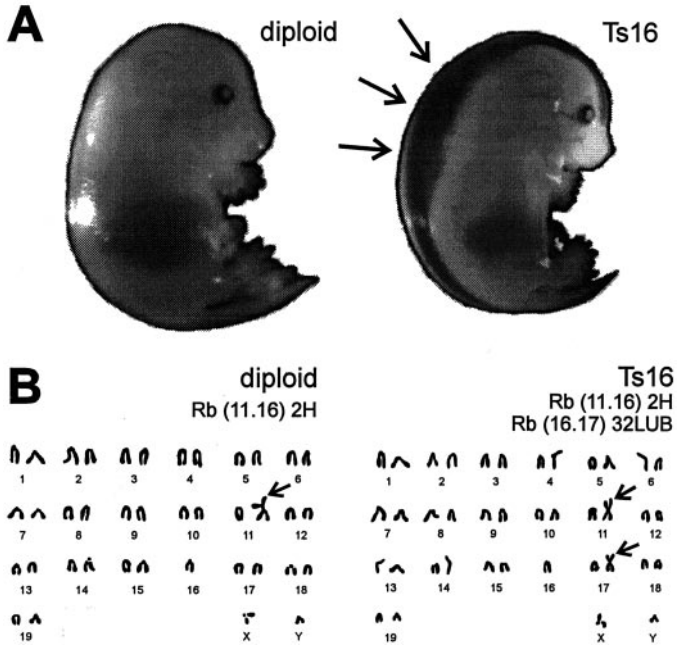

Figure 1. Diploid and Ts16 mice. *A*, Comparison between a 17-d-old diploid and Ts16 embryo. The Ts16 embryos were identified by characteristic edema of the neck (*arrows*), smaller size, and abnormal blood supply (hyperchrome liver). *B*, Karyotypings of diploid and Ts16 mice with Robertsonian translocation of chromosome 16. Karyotypings were made by using liver tissue. The second copy of chromosome 16 in the diploid mice is translocated to chromosome 11 (or 17; *arrow*). The karyotyping of Ts16 mice shows three copies of chromosome 16, with two Robertsonian translocations (to chromosomes 11 and 17; *arrows*).

ance will perturb normal citrate cycle metabolism, which because it is both a route of disposal and a source of the synthesis of glutamate and other neurotransmitters may have consequences for neurotransmitter synthesis and degradation (Hansford, 1985).

In this study we have investigated changes in intracellular $[Ca^{2+}]$ levels, mitochondrial membrane potential, and NAD(P)H after brief exposures to glutamate in cultured diploid and Ts16 hippocampal neurons. Our results demonstrate that Ts16 neurons display alterations in Ca^{2+} signaling and mitochondrial functions, such as the membrane potential and $NAD(P)^+$/NAD(P)H ratio.

MATERIALS AND METHODS

Preparation of cells. A breeding scheme was established between male mice with balanced bilateral Robertsonian translocations of chromosome 16 [Rb(16.17)32LUB and Rb(11.16)2H, kindly supplied by Professor H. Winking, Medizinische Hochschule Lübeck, Germany] that were mated with NMRI females (Bundesinstitut für gesundheitlichen Verbraucherschutz und Veterinärmedizin, BgVV, Berlin, Germany). Such matings result, on average, in one of three embryos with three copies of chromosome 16 (Gropp et al., 1975). Primary hippocampal cultures were prepared at gestation day 16 from Ts16 embryos and their diploid littermates (Banker and Cowan, 1977; Peacock et al., 1979). For this procedure, embryos were removed into ice-cold GBSS solution [Gey's balanced salt solution, containing (in mM): NaCl 136, KCl 5, $MgSO_4$ 0.3, NaH_2PO_4 1, $CaCl_2$ 1.5, $NaHCO_3$ 2.7, KH_2PO_4 0.22, $MgCl_2$ 1, glucose 5, pH 7.4] after the maternal animal was decapitated under deep ether anesthesia. The Ts16 embryos were identified by edema of the neck, smaller size, and abnormal blood supply as a result of a hyperchrome liver (Lane et al., 1996) and confirmed in initial experiments by karyotyping (Fig. 1). After preparation of diploid and Ts16 hippocampi, cells were separately dispersed by repetitive trituration with Pasteur pipettes and plated on poly-D-lysine-coated 12 mm coverslips ($5–6 \times 10^4$ cells/coverslip) and incubated at 36.5°C in a humidified atmosphere of 95% air and 5% CO_2 with minimum essential medium (MEM; Life Technologies, Eggenstein, Germany) supplemented with 10% (and after 3 d in culture, with 2%) heat-inactivated horse serum (Life Technologies), 12 mM glucose, 2 mM glutamine, serum extender MITO (Schubert, Schwandorf, Germany), 1 μM arabinofuranosid, and 2.5×10^4 U penicillin/streptomycin per milliliter culture medium. Cells were maintained in culture for up to 4 weeks. Most experimental data were obtained within 2–21 d in culture.

Fluorescence measurements. Microfluorimetric experiments were performed using an imaging system based on a Zeiss Axioskop microscope with 10× and 40× water-immersion objectives (numerical aperture, 0.3 and 0.75, respectively; Zeiss, Jena, Germany), a xenon light source with a combination of two monochromators [Photon Technology Instruments (PTI), Wedel, Germany], a charge-coupled device camera (Hamamatsu, Herrsching, Germany), and a photomultiplier (Seefelder Messtechnik, Seefeld, Germany). Image hardware was controlled by an IBM-compatible computer running commercial software developed by PTI.

The cells were incubated in media containing the different fluorescence dyes (Molecular Probes Europe, Leiden, Netherlands) for 10–15 min at 36.5°C. After the cells were washed for 15 min at 36.5°C using fresh media, the dyes were retained for 3–5 hr. Rhodamine 123 (Rh123) was dissolved in aqueous solution (0.1% ethanol), and cells were loaded by incubation with a final concentration of 10 μg of dye per 1 ml of culture medium (26.3 μM). Rh123 fluorescence was excited at 490 nm and measured above 530 nm using a 515 nm dichroic mirror and a 530 long-pass filter. To differentiate between living and dead cells, double-staining with the intercalating dyes acridine orange (AO) (5 μM) and ethidium bromide (EB) (10 μM) dissolved in aqueous solution were used. The two dyes were applied simultaneously, excited at 490 nm, and measured using an optical combination of a 505 nm dichroic mirror and a 515 nm long-pass filter. The membrane-permeable AO interacts in living cells with DNA (emission 515 nm, green) and RNA (emission 650 nm, red), whereas the membrane-impermeable EB binds only in dead cells to DNA (emission 605 nm, red) (Oyama et al., 1994) (Fig. 2*B*). For measurements of $[Ca^{2+}]_i$, the acetoxymethyl (AM) ester of fura-2 (final concentration 2–3 μM) was used. Fura-2 was excited at 340 nm and 380 nm, and fluorescence was measured at 510 nm. The calibration of the fura-2 fluorescence signal was performed by using an *in vitro* calibration procedure. Fura-2 (1 μM) as the free acid was added to saline containing Ca^{2+}-EGTA buffers, giving minimum and saturating levels of Ca^{2+} and hence the minimum (R_{min}) and maximum (R_{max}) fluorescence ratios and also the ratio of the Ca^{2+}-free and Ca^{2+}-saturated fluorescence excited at 380 nm (β), required for the equation (Grynkiewicz et al., 1985): $[Ca^{2+}]_i = K_D\beta(R - R_{min}/R_{max} - R)$. The value of the *in vitro* dissociation constant K_D in the described system was close to reported data [224 nM (Duchen, 1992a)]. Autofluorescence of NAD(P)H was monitored by exciting at 360 nm and measuring light emitted above 400 nm using a 390 nm dichroic mirror and a 400 nm long-pass filter (Aubin, 1979; Duchen, 1992a).

For all fluorescence measurements, neurons were differentiated from glial cells in phase-contrast illumination [relatively small phase-dark cell body (10–15 μm) with fine processes; see Fig. 2*A*].

Drugs and solutions. During the experiments, cells were continuously superfused with oxygenated (95% O_2, 5% CO_2) artificial CSF (ACSF), containing (in mM): NaCl 124, KCl 3, NaH_2PO_4 1.25, $MgSO_4$ 2, $CaCl_2$ 2, $NaHCO_3$ 26, glucose 10, pH 7.35. Sodium glutamate (Sigma, Deisenhofen, Germany) was applied with concentrations of 10 μM to 1 mM. For a number of experiments, the following drugs were added to culture media: 30 μM 2-amino-5-phosphonovalerate (APV), 10 μM 2,3-dihydroxy-6-nitro-7-sulfamoylbenzo(F) quinoxalin (NBQX), 50 μg/ml tocopherol (vitamin E) (all from Sigma), and 0.5–1.5 μM cyclosporin A (Biomol, Hamburg, Germany). In some experiments the solution was changed to a nominally Ca^{2+}-free saline solution. In these cases, 2 mM $MgSO_4$ substituted 2 mM $CaCl_2$. All experiments were performed at 30–32°C.

Data acquisition. Living neurons were identified by phase-contrast illumination and AO/EB double staining. Moreover neurons were characterized in phase-contrast illumination measurements by a relatively small, phase-dark cell body (10–15 μm) with fine processes and therefore could be easily differentiated from glial cells. If it was not clear whether the fluorescent nucleus was from a neuron or an underlying glial cell, the subfield was excluded from analysis. The AO-positive and EB-negative neurons were counted in 20–30 subfields (diameter 400 μm) of each culture dish. To approximate the total number of living neurons on the dish, the subfield mean value of AO-positive and EB-negative neurons

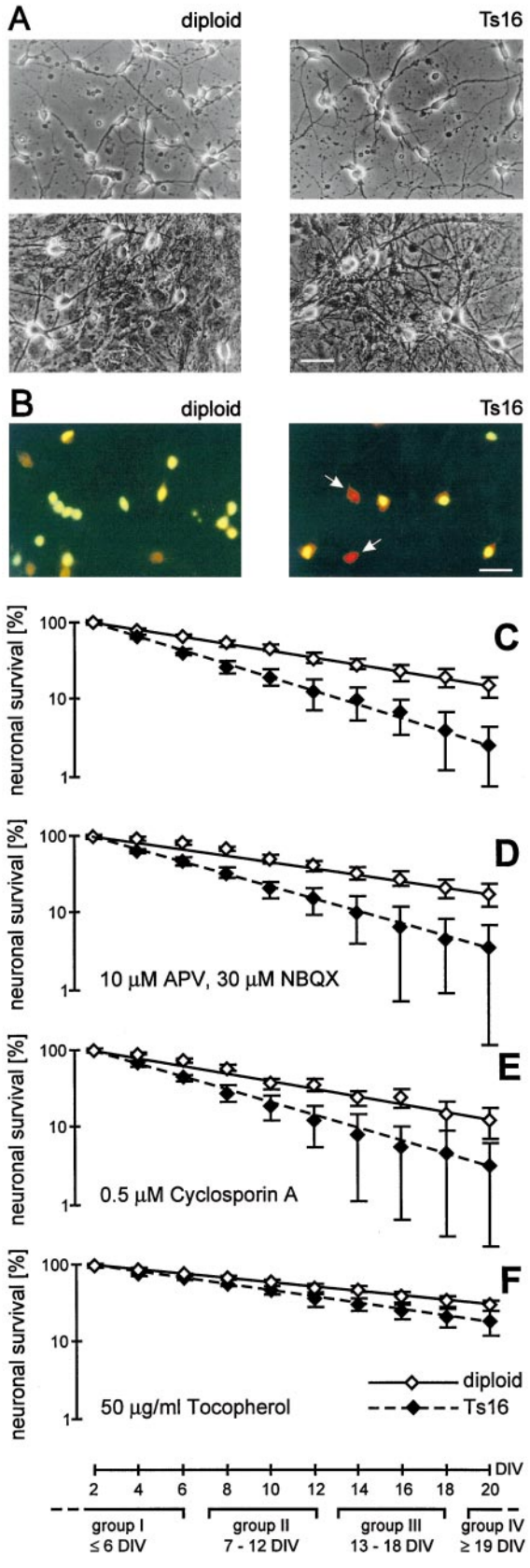

Figure 2. Live–dead assay of cultured diploid and Ts16 neurons. *A*, Phase-contrast micrographs of hippocampal diploid (*left*) and Ts16 (*right*) cultures after 2 (*top images*) and 12 (*bottom images*) DIV. No morphological differences could be observed between diploid and Ts16 neurons at any age in culture. In phase-contrast illumination, neurons were characterized by a relatively small phase-dark cell body (10–15 μm) with fine processes and therefore could be easily differentiated from confluent glial cells, which can be seen in the background. Scale bar, 30 μm. *B*, AO/EB double staining for characterization of live–dead neurons in diploid (*left*) and Ts16 (*right*) cultures. Cells with intact membrane show *yellow-green* nuclei as a result of DNA interaction with the membrane-permeable AO. Cytosolic RNA in these cells can be colored red by AO. Interactions between plasma membrane impermeable EB and DNA result in a dark red-colored nucleus. Therefore, cells with a dark red nucleus manifest a damaged plasma membrane and were characterized as dead neurons. In Ts16, culture *arrows* indicate ethidium bromide-positive neurons, which were counted as dead neurons. If under phase-contrast illumination it was difficult to discriminate whether the fluorescent nucleus was from a neuron or underlying glial cell, the subfield was excluded from analysis. Scale bar, 30 μm. *C*, Semilogarithmic plot of a linear regression of survival as a function of days *in vitro* (*DIV*) of diploid (*open squares, solid line*) and Ts16 (*closed squares, dashed line*) hippocampal neurons. Live neurons were counted every second day *in vitro* by using phase-contrast microscopy and AO/EB double staining. The amount of surviving neurons over time in culture could be fitted using a single-exponential function, i.e., the probability of spontaneous neuronal cell death did not change over time in both diploid and Ts16 cultures. However, Ts16 neurons die more than twice as fast as diploid neurons. Data are mean ± SEM of three coverslips out of each of four different preparations. The slope of the fits is significantly different at $p < 0.001$. *D*, Neuronal survival after addition of 30 μM APV and 10 μM NBQX. Compared with control conditions, the neuronal death rate constant showed no significant change between diploid and Ts16 cultures. *E*, In the presence of 0.5 μM cyclosporin A, the neuronal death rate constant in both diploid and Ts16 cultures showed no significant change in comparison to control conditions. *F*, In the presence of 50 μg/ml tocopherol, neuronal survival in both diploid and Ts16 cultures increased significantly. Neuronal cell death rate constant in diploid cultures showed a significant reduction (vs control conditions with $p < 0.01$). In Ts16 cultures the neuronal death rate constant was halved in comparison to control conditions ($p < 0.001$).

was multiplied by the ratio of the coverslip surface (113.10 mm^2) and subfield surface (0.13 mm^2).

CCD camera image frames were usually obtained from groups of 3–10 optically identified neurons, digitized with 8 bits (spatial resolution up to 512 × 480 pixels), and stored on the computer hard disk. The recording frequency was adapted for the different experiments at between 0.5 and 300 images/sec. For the off-line analysis, fluorescence signals from single neurons were measured by using median values from individually adjusted regions of interest. These data were finally presented as the change in fluorescence signal from the baseline level $\Delta F/F_0$ (Rh123) or as an absolute change of Ca^{2+} concentration (fura-2).

Photomultiplier NAD(P)H measurements were acquired from clusters consisting of 10–15 optically identified neurons. The recording frequency was between 2 and 10 Hz. The data were normalized to change in autofluorescence signal from the baseline level $\Delta F/F_0$.

Statistics. All values are given as means ± SEM. Statistical differences of individual data points were assessed by using a one-way ANOVA followed by Bonferroni/Dunn comparison. To analyze statistical differences in spontaneous neuronal cell death, the slopes of the linear regression of the semilogarithmical plot, e.g., the death rate constants, were assessed by using a one-way ANOVA followed by Bonferroni/Dunn comparison.

RESULTS

Tocopherol inhibits spontaneous neuronal cell death in diploid and Ts16 cultures

For a quantitative analysis of spontaneous neuronal cell death in diploid and Ts16 cultures, the total number of surviving neurons on coverslips was counted every second day starting at 2 d *in vitro* (DIV). For every second DIV, at least two coverslips from three different preparations were evaluated by counting the number of AO-positive/EB-negative (living) and AO-negative/EB-positive (dead) neurons in 20–30 subfields of the culture dish. Out of these data the total numbers of living and dead neurons on the cover-

slips were approximated. For all experimental sets, the percentage decline of surviving neurons over time in culture could be fitted using a single-exponential function $f(t) \sim \exp(\lambda t)$. Therefore, the death of each single neuron can be taken as an independent stochastic event (Dubinsky et al., 1995). In a semilogarithmical plot, the death rate constant λ results from the slope of the linear regression line. Figure 2*C–F* shows the mean values ± SEM in percentage of living neurons in control conditions and with the addition of APV/NBQX, cyclosporin A, and tocopherol to the culture medium.

Under control conditions (Fig. 2*C*), the linear fits indicate a death rate constant for diploid neurons of 10.1 ± 0.5% per day and 22.7 ± 0.9% per day for Ts16 neurons (slopes of the fits are significantly different at $p < 0.001$). Thus, Ts16 neurons die more than twice as fast as diploid neurons under otherwise identical culture conditions. The addition of glutamate receptor antagonists APV (30 μM) and NBQX (10 μM) to the culture medium (Fig. 2*D*) had no significant effect on the survival of both diploid and Ts16 neurons. Compared with the situation under control conditions, the death rate constant did not change in diploid (10.2 ± 1.2%) or Ts16 cultures (18.8 ± 2.3%). With the addition of 0.5 μM cyclosporin A (Fig. 2*E*), an inhibitor of the mitochondrial permeability transition, analogous results were found: the neuronal death rate constant showed no significant change in diploid (11.9 ± 1.1%) and Ts16 cultures (19.4 ± 1.4%) in comparison to control conditions. Only the application of 50 μg/ml tocopherol (Fig. 2*F*), an antioxidant binding preferentially to the plasma membrane, led to a significant increase in neuronal survival. Whereas the neuronal death rate constant in diploid cultures showed a reduction to 6.6 ± 0.8%, the death rate constant in Ts16 cultures was halved (9.4 ± 1.1%) in comparison to control conditions. The observed reduction in neuronal death rate constant was significant in both diploid ($p < 0.01$) and Ts16 cultures ($p < 0.001$) compared with the situation under control conditions. Furthermore, the addition of tocopherol to the culture medium abolished the significant difference between the neuronal death rate constant in diploid and Ts16 cultures observed under control conditions and in the presence of APV/NBQX or cyclosporin A.

Inhibition of the mitochondrial permeability transition prevents glutamate-induced neuronal death in diploid and Ts16 neurons

To study differences in the vulnerability of cultured hippocampal diploid and Ts16 neurons to excitotoxic damage, we applied of 50 μM glutamate for 60 min to the culture medium. Before and every 2 hr after glutamate stimulation, the number of AO-positive/EB-negative and AO-negative/EB-positive neurons was evaluated from at least two coverslips from three different preparations. The experiments were performed on diploid and Ts16 cultures between 8 and 20 DIV. The total number of living as well as dead neurons on the coverslips was approximated as described above.

Figure 3*A* shows the neuronal survival in diploid and Ts16 cultures for 24 hr under control conditions. The increased death of Ts16 neurons compared with diploid neurons was already recognizable but not significantly different at this time (24 hr: diploid 95.2 ± 4.2%, Ts16 85.7 ± 6.7%). The application of 50 μM glutamate for 60 min was followed by a strong intensification of neuronal death in diploid and Ts16 cultures. Twenty-four hours after the glutamate stimulation, the proportion of surviving neurons decreased to 66.5 ± 6.6% in diploid and 30.7 ± 7.6% in Ts16 cultures (diploid vs Ts16, $p < 0.001$) (Fig. 3*B*). In comparison to diploid cultures and the results under control conditions, the neuronal death in Ts16 cultures was found to be enhanced even 24 hr after glutamate application.

The glutamate-induced intensification of neuronal death was dependent on the extracellular Ca^{2+} concentration. After nominal removal of Ca^{2+} from the extracellular medium, the increase in neuronal cell death that followed the application of 50 μM glutamate was widely suppressed in both diploid and Ts16 cultures (24 hr: diploid 81.9 ± 6.3%, Ts16 66.5 ± 7.3%) (Fig. 3*C*). Diploid and Ts16 neurons were also successfully protected against glutamate-induced excitotoxicity in the presence of the glutamate receptor antagonists APV (30 μM) and NBQX (10 μM) (24 hr: diploid 87.8 ± 5.7%, Ts16 78.8 ± 7.4%) (Fig. 3*D*). The removal of extracellular Ca^{2+} and the presence of APV/NBQX protected neurons from glutamate-induced increases of $[Ca^{2+}]_i$ (Choi, 1988b; Bleakman et al., 1993). Elevation of $[Ca^{2+}]_i$ leads to a reduction and subsequent collapse of mitochondrial membrane potential (Duchen, 1992b). To study the significance of $[Ca^{2+}]_i$ and mitochondrial function for neuronal survival, we investigated the effects of cyclosporin A, an inhibitor of mitochondrial permeability transition (Starkov et al., 1994; Pastorino et al., 1995; Nicolli et al., 1996). Cyclosporin A delays mitochondrial depolarization (Nieminen et al., 1996) and presumably prevents glutamate-induced collapse of mitochondrial membrane potential (Schinder et al., 1996). The presence of 1.5 μM cyclosporin A protected diploid and Ts16 neurons to a similar extent as did nominally Ca^{2+}-free or APV/NBQX-containing culture medium against glutamate-induced increase in neuronal cell death (24 hr: diploid 83.7 ± 6.5%, Ts16 72.8 ± 7.9%) (Fig. 3*E*). Tocopherol, in contrast to the protecting effects in unstimulated cultures, had only minor effects on the glutamate-induced increase in the death of diploid and Ts16 neurons. In the presence of 50 μg/ml tocopherol, 24 hr after the application of 50 μM glutamate, 69.6 ± 5.4% and 45.3 ± 7.9% live neurons were counted in diploid and Ts16 cultures, respectively (diploid vs Ts16, $p < 0.01$) (Fig. 3*F*). In Ts16 cultures, tocopherol reduced the neuronal cell death in comparison to the glutamate-only control condition (amount of surviving Ts16 neurons 24 hr after glutamate application without vs with tocopherol = $p < 0.01$).

Age-dependent increase of basal $[Ca^{2+}]_i$ in Ts16 neurons

The age dependence of basal $[Ca^{2+}]_i$ and the other investigated parameters were analyzed by subdividing our culture into four age groups: I, ≤6 DIV; II, 7–12 DIV; III, 13–18 DIV; IV, ≥19 DIV. Figure 4 illustrates the intracellular Ca^{2+} levels monitored with fura-2 AM for diploid and Ts16 neurons in these four different age groups. For each age group of diploid and Ts16 cultures, at least 600 neurons out of three separate cultures (four different coverslips with 50–60 neurons for each culture) were studied. Neurons with incomplete dye loading (<20 nM $[Ca^{2+}]_i$) and dying neurons (>500 nM $[Ca^{2+}]_i$) were excluded from the analysis (diploid 4.1%, Ts16 5.8% of all measured neurons). In the youngest age group (up to 6 DIV), the basal $[Ca^{2+}]_i$ did not significantly differ between diploid (group I: 93.67 ± 3.57 nM) and Ts16 neurons (group I: 77.51 ± 3.71 nM). The basal $[Ca^{2+}]_i$ in age group II was unchanged in diploid neurons (96.99 ± 1.81 nM) and increased in Ts16 neurons (113.08 ± 3.58 nM). Ts16 neurons of age group II showed a larger basal $[Ca^{2+}]_i$ in comparison to diploid neurons, but the difference was not significant. With further aging, the basal $[Ca^{2+}]_i$ was stable in diploid neurons but increased steadily in Ts16 neurons. The $[Ca^{2+}]_i$ of Ts16 neurons

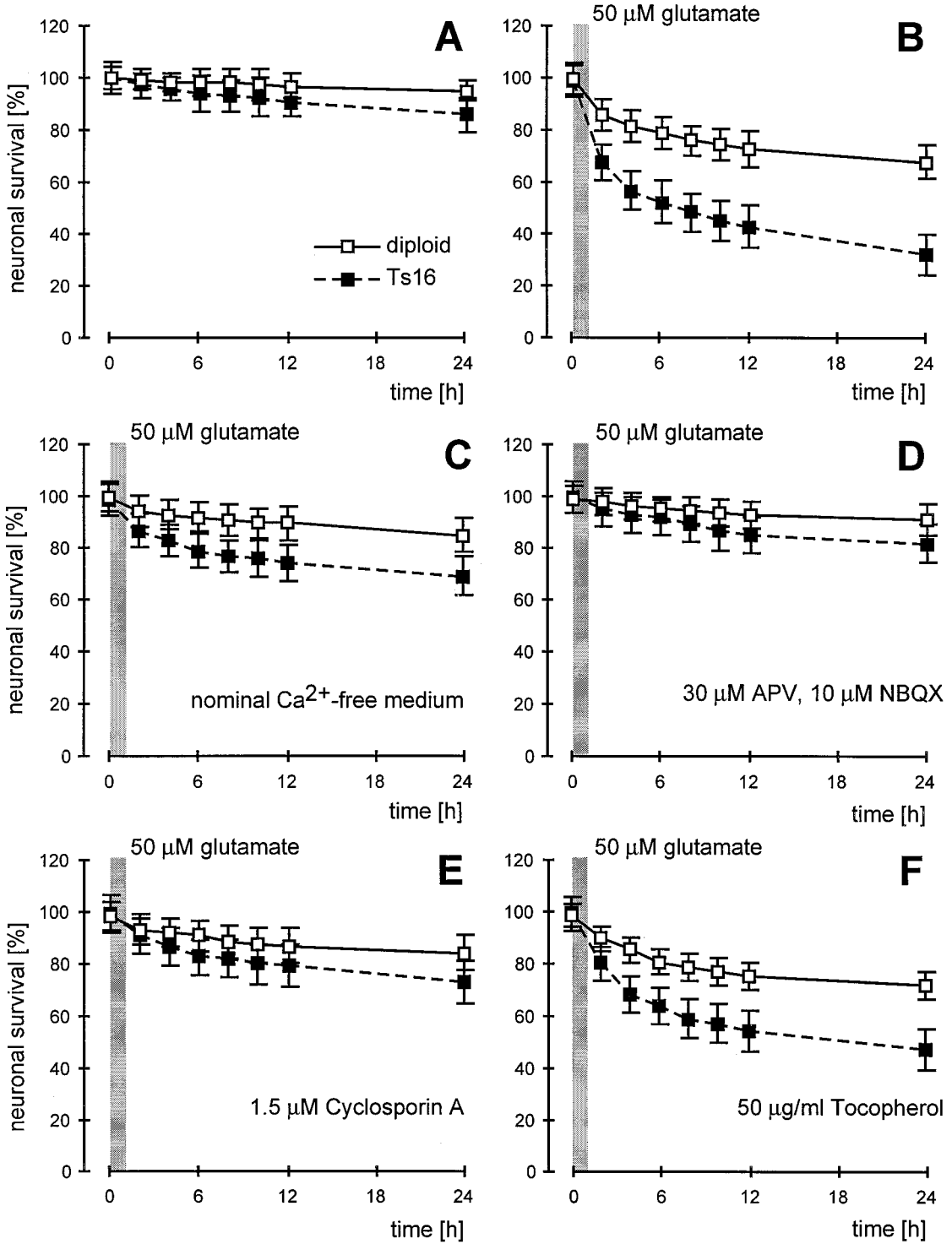

Figure 3. Glutamate-induced neuronal death in diploid and Ts16 cultures. Neuronal survival in diploid (*open squares, solid line*) and Ts16 (*closed squares, dashed line*) cultures under control conditions and within 24 hr after the application of glutamate. Glutamate remained in the culture media for 60 min; subsequently cells were rinsed with fresh (glutamate-free) media. Each data point in the figures represents at least 100 neurons (8–20 DIV) out of three different preparations. *A*, Neuronal survival in diploid and Ts16 neurons under control conditions in the absence of glutamate. Ts16 cultures showed an increased neuronal cell death in comparison with diploid cultures, but the difference was not significant after 24 hr. *B*, The application of 50 μM glutamate for 60 min results in a reduction of neuronal survival in both diploid and Ts16 cultures. Moreover, the amount of surviving neurons was significantly decreased in Ts16 cultures in comparison to diploid cultures (24 hr after glutamate application, $p < 0.001$). *C*, In nominal Ca^{2+}-free medium, diploid and Ts16 neurons were protected against glutamate-induced neurotoxicity. There was no significant reduction in the amount of surviving neurons in both diploid and Ts16 cultures 24 hr after the application of 50 μM glutamate for 60 min in comparison to control conditions. *D*, Neuronal survival after the application of 50 μM glutamate for 60 min in the presence of the NMDA-receptor antagonist APV (30 μM) and the non-NMDA-receptor antagonist NBQX (10 μM). Both diploid and Ts16 neurons were successfully protected against the two components of glutamate-induced neurotoxicity: neuronal swelling caused by Na^+ and Cl^- influx via non-NMDA receptors and delayed neuronal degeneration as a result of Ca^{2+} *(Figure legend continues)*

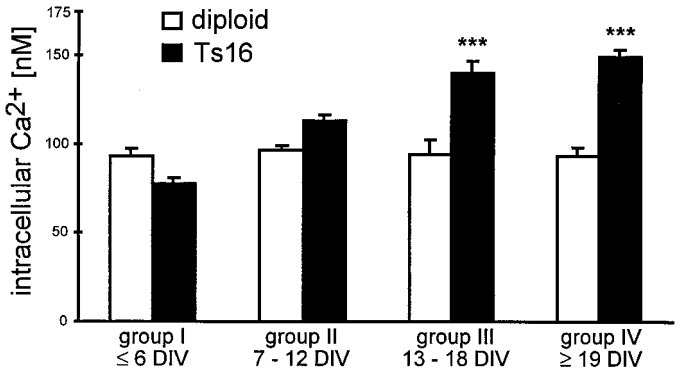

Figure 4. Basal $[Ca^{2+}]_i$ levels in diploid and Ts16 neurons. Intracellular basal $[Ca^{2+}]_i$ for diploid (*open bars*) and Ts16 (*closed bars*) neurons out of the different age groups indicated by fura-2 AM (2–3 μM). Diploid neurons showed a nearly steady basal $[Ca^{2+}]_i$, whereas in Ts16 neurons the basal $[Ca^{2+}]_i$ increased constantly during the observed time interval. After 2 weeks in culture the basal $[Ca^{2+}]_i$ in Ts16 neurons was significantly raised in comparison to diploid neurons (***$p < 0.001$). Data are mean ± SEM of 12 experiments; for each age group at least 600 neurons were counted.

of groups III and IV was significantly increased in comparison to diploid control neurons (group III: diploid 94.37 ± 8.3 nM, Ts16 140.44 ± 6.5 nM, $p < 0.001$; group IV: diploid 93.24 ± 5.36 nM, Ts16 149.76 ± 3.37 nM, $p < 0.001$).

Age-dependent changes in potassium- and glutamate-induced rises of $[Ca^{2+}]_i$ in diploid and Ts16 neurons

Fura-2 AM-loaded diploid and Ts16 neurons were exposed for 10 sec to 50 mM K^+ or 100 μM glutamate. Changes in $[Ca^{2+}]_i$ were investigated by obtaining 340/380 nm ratio images with one image per 2 sec (0.5 Hz). Figure 5 shows plots of the average changes in $[Ca^{2+}]_i$ after stimulation with K^+ (at least 30 neurons for each age group out of three different preparations) (Fig. 5*A*) or glutamate (45 neurons for each age group out of six different preparations) (Fig. 5*B*).

The application with 50 mM K^+ for 10 sec induced a rapid increase in $[Ca^{2+}]_i$ in all age groups of both diploid and Ts16 neurons, presumably by depolarization of the plasma membrane and activation of voltage-gated Ca^{2+} channels. The maximum rise in $[Ca^{2+}]_i$ showed only minor changes in the different age groups (diploid 496–558 nM; Ts16 521–598 nM). The $[Ca^{2+}]_i$ increase in Ts16 neurons showed a slight delay in comparison to diploid neurons in all age groups. Furthermore, the recovery of $[Ca^{2+}]_i$ in Ts16 neurons was prolonged in comparison to diploid neurons of the same age groups. Figure 5*C* illustrates that the time integral of the $[Ca^{2+}]_i$ signal after the stimulation with K^+ increases as a function of age in both diploid and Ts16 neurons. The total $[Ca^{2+}]_i$ integral in Ts16 neurons was significantly augmented in all age groups in comparison to diploid control neurons.

In contrast to the stimulation with K^+, the glutamate-induced increase in $[Ca^{2+}]_i$ showed a strong growth with age in culture that corresponds to the expression of glutamate receptors by cultured neurons. Thus, cultured hippocampal neurons become sensitive to NMDA after 7–10 DIV (Mattson and Kater, 1988, 1989). Therefore the rise in $[Ca^{2+}]_i$ during and after exposure to glutamate increased with the age of the neurons. Interestingly, the amplitude of $[Ca^{2+}]_i$ increase in each age group was somewhat larger in the diploid neurons than in Ts16 neurons (Table 1). In contrast to diploid control neurons, Ts16 neurons show both a slower rise time of $[Ca^{2+}]_i$ and a slower recovery to baseline. The rise time of $[Ca^{2+}]_i$ was nearly constant with age in diploid and Ts16 neurons. Decay times of $[Ca^{2+}]_i$ became longer with days *in vitro* both in diploid and Ts16 neurons but were significantly longer in Ts16 neurons than in diploid neurons in all age groups. The $[Ca^{2+}]_i$ declines with at least two different time constants. In Table 1 both time constants, τ_{fast} and τ_{slow}, are quantified for the different age groups. There was an elevation in the integral of $[Ca^{2+}]_i$ signal over time in Ts16 neurons as compared with diploid neurons that was independent of the initial rise in $[Ca^{2+}]_i$ (Fig. 5*D*). This is caused by a slowed Ca^{2+} recovery kinetic that is also reflected in the significant elevated time constants of both phases of Ca^{2+} recovery in most age groups of Ts16 cultures. Only τ_{fast} of age group II showed no significant difference between diploid and Ts16 neurons (Table 1).

Delayed recovery of mitochondrial membrane potential after glutamate-induced depolarization in Ts16 neurons

Mitochondria are the only organelles known to have a significant negative membrane potential (Chen, 1989). This potential is driven by the respiratory electron transport chain and is required for the synthesis of ATP. The lipophilic cation rhodamine 123 (Rh123) is accumulated by mitochondria in response to the negative membrane potential (Johnson et al., 1980; Chen, 1989). Binding of the accumulated dye molecules to the mitochondrial matrix is associated with a fluorescence quench (Emaus et al., 1986). Depolarization of the mitochondrial membrane allows redistribution of the dye from the mitochondria into the cytosol. This event is correlated with an increase in the Rh123 fluorescence signal. In contrast, hyperpolarization of the mitochondrial membrane will increase the uptake of the dye from the cytosol into the mitochondria and thereby increase the fraction of quenched dye. Thus hyperpolarization of mitochondrial membrane will decrease the Rh123 fluorescence signal (Duchen et al., 1993). In this study, the distribution and quenching of the Rh123 fluorescent signal was used to monitor changes in mitochondrial membrane potential.

It has been reported previously that intracellular Ca^{2+} accumulation will depolarize mitochondrial membrane potential and thereby increase the Rh123 signals (Duchen, 1992b). Figure 6 illustrates that the application of glutamate leads to a depolarization of the mitochondrial membrane in the presence of extracellular Ca^{2+} in both diploid and Ts16 neurons. This effect was lost when glutamate was applied in the presence of nominally Ca^{2+}-

←

influx via NMDA receptor (Choi, 1988b, 1995). *E*, The presence of 1.5 μM cyclosporin A prevented the augmentation of neuronal death after the application of 50 μM glutamate in diploid and Ts16 cultures. The amount of surviving neurons showed no significant reduction in both diploid and Ts16 cultures 24 hr after the application of glutamate in comparison to control conditions. This implicates the participation of the Ca^{2+}-induced mitochondrial membrane permeability transition in the glutamate-induced neuronal degeneration. *F*, The presence of 50 μg/ml tocopherol protected diploid and Ts16 cultures against spontaneous neuronal cell death. It was less effective against glutamate-induced neuronal cell death. Only the neuronal cell death that followed the application of glutamate in Ts16 cultures was significantly reduced in the presence of tocopherol (amount of surviving Ts16 neurons 24 hr after glutamate application without vs with tocopherol, $p < 0.01$). This may point to an increased generation and participation of ROS molecules, independent from glutamate-induced neurotoxicity, in neuronal degeneration in Ts16 cultures.

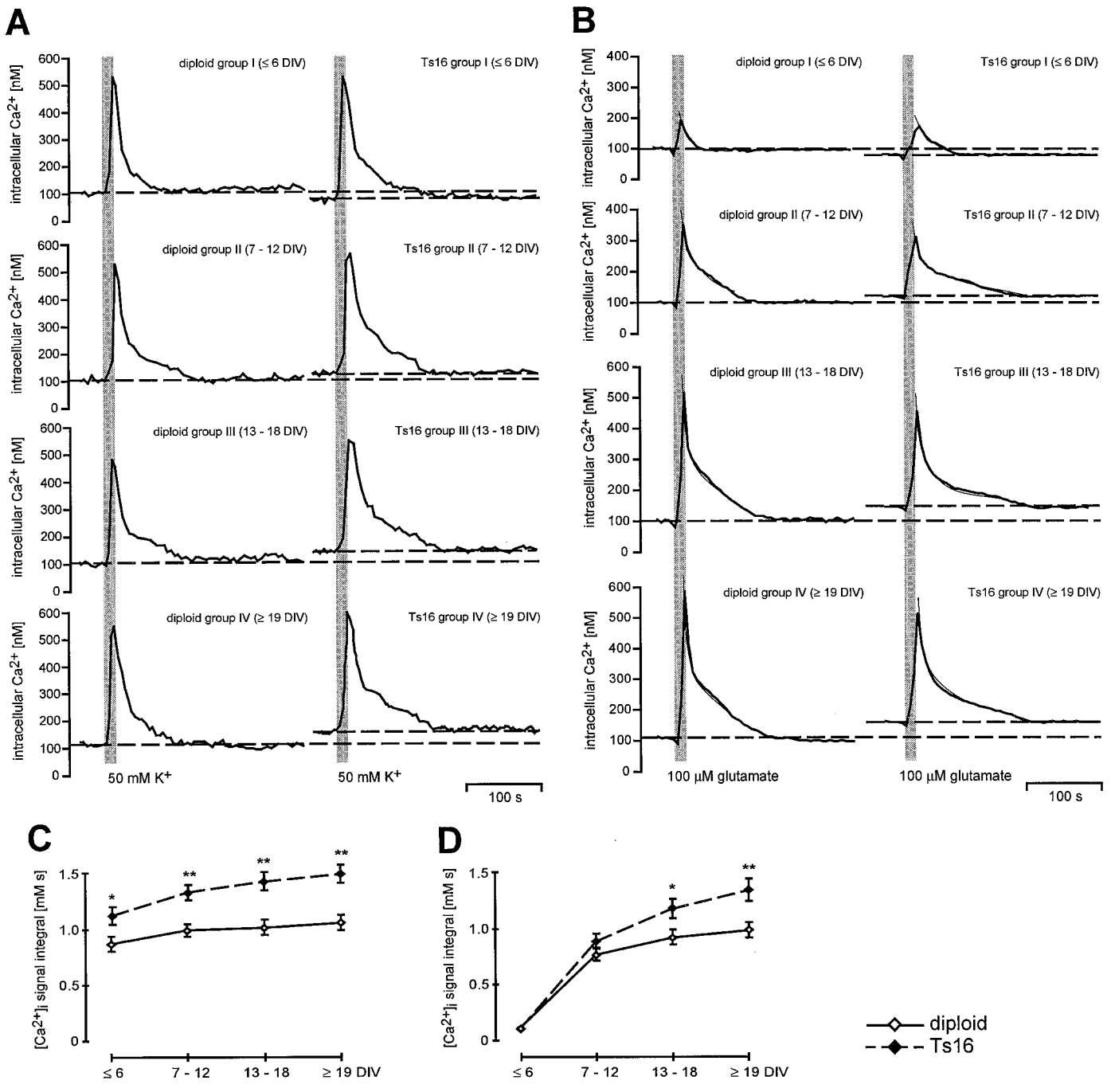

Figure 5. $[Ca^{2+}]_i$ changes after exposure to glutamate and potassium. *A*, Intracellular $[Ca^{2+}]_i$ increase and recovery after depolarization of diploid (*left*) and Ts16 (*right*) neurons using K^+. Cultures of the different age groups were stained with 2–3 μM fura-2 AM for 15 min. For measurements, cultures were suspended in dye-free ACSF at 30–32°C and exposed to 50 mM K^+ for 10 sec. The plots are based on the means of six experiments for each age group. *B*, Intracellular $[Ca^{2+}]_i$ increase and recovery after application of 100 μM glutamate for 10 sec in diploid (*left*) and Ts16 (*right*) neurons. The plots are based on the means of six experiments for each age group. The *dashed line* represents the basal $[Ca^{2+}]_i$ level and shows the differences in basal $[Ca^{2+}]_i$ between diploid and Ts16 neurons. The $[Ca^{2+}]_i$ recovery was fitted to a double-exponential function (*hairline*; see Table 1). The $[Ca^{2+}]_i$ signal integral quantifies the Ca^{2+} influx and was calculated for diploid (*open squares, solid line*) and Ts16 (*closed squares, dashed line*) neurons of all age groups. For the calculation, parameters from the double-exponential fit were used. The integral was calculated in the interval between the time of $[Ca^{2+}]_i$ maximum and the first time that the intracellular calcium concentration reached the initial basal $[Ca^{2+}]_i$ in Ts16 cultures. Therefore, the results are useful for the estimation of $[Ca^{2+}]_i$ recovery. Diploid neurons, in contrast to Ts16 neurons, displayed a more flattened course of the $[Ca^{2+}]_i$ signal integral as a function of all age groups. Thus, Ts16 neurons manifested a retarded $[Ca^{2+}]_i$ recovery after K^+- and glutamate-induced $[Ca^{2+}]_i$ increase. *C*, $[Ca^{2+}]_i$ signal integral after brief application of 50 mM K^+. $[Ca^{2+}]_i$ increased via voltage-activated channels in diploid and Ts16 neurons. The $[Ca^{2+}]_i$ signal integral in Ts16 neurons was significantly increased compared with diploid neurons ($^*p < 0.05$; $^{**}p < 0.01$) in all age groups. *D*, $[Ca^{2+}]_i$ signal integral after brief application of 100 μM glutamate. $[Ca^{2+}]_i$ increased via the NMDA receptor-gated channels in diploid and Ts16 neurons. The $[Ca^{2+}]_i$ signal integral showed an increase with age in culture that corresponds to the expression of glutamate receptors ($^*p < 0.05$; $^{**}p < 0.01$).

Table 1. $[Ca^{2+}]_i$ increase and recovery after application with glutamate

		Diploid				Ts16			
Age group		*n*	Maximum $[Ca^{2+}]_i$ (nM)	τ_{fast} (1/sec)	τ_{slow} (1/sec)	*n*	Maximum $[Ca^{2+}]_i$ (nM)	τ_{fast} (1/sec)	τ_{slow} (1/sec)
I	≤6 DIV	52	184.61 ± 14.23	10.75 ± 0.20	10.53 ± 0.20	47	170.15 ± 17.41	20.41 ± 0.01***	19.61 ± 0.01***
II	7–12 DIV	57	349.21 ± 12.43	6.13 ± 0.07	4.15 ± 0.05	51	303.40 ± 14.79	6.34 ± 0.04	4.61 ± 0.18*
III	13–18 DIV	69	513.48 ± 11.91	5.68 ± 0.26	3.34 ± 0.04	68	452.53 ± 15.33*	6.94 ± 0.63*	4.93 ± 0.10**
IV	≥19 DIV	58	580.00 ± 14.12	5.49 ± 0.17	3.07 ± 0.05	48	503.20 ± 18.24**	6.25 ± 0.19*	3.66 ± 0.06**

Data from glutamate-induced $[Ca^{2+}]_i$ increase in diploid and Ts16 hippocampal neurons for all age groups. The first column summarizes the number of analyzed neurons (*n*, out of six different cultures). The second column represents the maximum value of $[Ca^{2+}]_i$ after the glutamate stimulus (maximum $[Ca^{2+}]_i$, mean value ± SEM in nanomols). The time constants τ_{fast} and τ_{slow} given in the third and fourth column result from double-exponential fit: $f(t) = A + B \cdot \exp(-(t/\tau_{fast})) + C \cdot \exp(-(t/\tau_{slow}))$ to the $[Ca^{2+}]_i$ recovery (Fig. 4). Asterisks represent statistical significance between diploid and Ts16 data within each age group (*$p < 0.05$; **$p < 0.01$; ***$p < 0.001$).

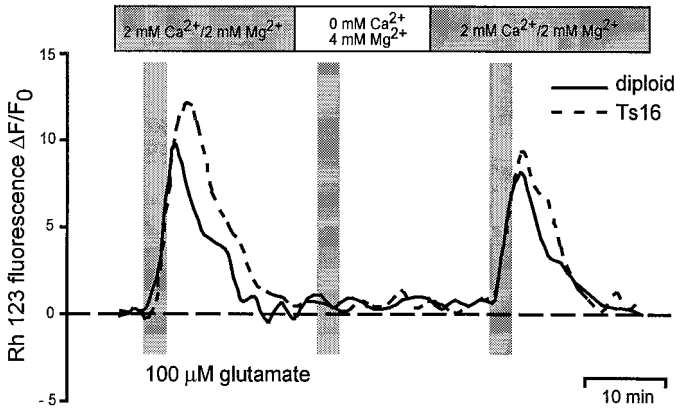

Figure 6. Ca^{2+}-dependent depolarization of mitochondrial membrane. Diploid and Ts16 cultures were incubated with Rh123 (10 μg/ml) for 15 min. Cells were washed and suspended for measurements in dye-free ACSF at 30–32°C. For the indicated period, the superfusion medium was changed to nominal Ca^{2+}-free medium (substituted with Mg^{2+}; see Materials and Methods). During this period, application of 100 μM glutamate for 150 sec had no effect on the mitochondrial membrane potential. After a return to Ca^{2+}-containing medium, the response recovered. This was observed for both diploid (*solid line*) and Ts16 (*dashed line*) neurons. Furthermore, diploid and Ts16 neurons showed, after reapplication of Ca^{2+}-containing medium, a decrease in glutamate-induced depolarization of the mitochondrial membrane. This decrease was also observed during repeated glutamate stimulations without application of nominally Ca^{2+}-free media (data not shown).

free medium. The effect was reversible after reapplication of Ca^{2+}-containing medium and did not depend on age. The Ts16 neurons showed a larger increase in the Rh123 signal and depolarization of mitochondrial membrane in comparison to diploid neurons in all age groups. As a result, in Ts16 neurons we observed an elevated depolarization of mitochondrial membranes despite the reduced initial $[Ca^{2+}]_i$ peak.

Figure 7 illustrates the depolarization of mitochondrial membranes, as monitored by Rh123, during application of 10 μM, 100 μM, and 1 mM glutamate to diploid and Ts16 neurons in all age groups. The illustrated plots are based on mean values from at least 24 Ts16 and 36 diploid neurons out of three different cultures for each age group. The glutamate stimulus of 30 sec was immediately followed by a depolarization of the mitochondrial membrane and a relatively slow recovery of polarization to baseline. In the first age group (≤6 DIV), Ts16 neurons showed a smaller but not significant difference in the maximum Rh123 signal in contrast to diploid neurons. In age group II (7–12 DIV), maximum Rh123 signal was doubled for glutamate concentrations >50 μM in Ts16 neurons and diploid neurons. In comparison to diploid control neurons, Ts16 neurons of age groups III and IV (≥13 DIV) were characterized by a larger maximum Rh123 signal that showed an elevation with age in culture. Figure 7*B* summarizes concentration–response curves for maximum Rh123 signal increase after glutamate stimulation for all age groups and glutamate concentrations. The concentration–response curves leveled off above 0.5 mM glutamate in all age groups and in both cell types. After 2 weeks in culture (group III, 13–18 DIV), Ts16 neurons show a significantly larger maximum Rh123 increase compared with diploid neurons after stimulation with 50, 75, and 100 μM glutamate (Table 2). In older Ts16 neurons (group IV, ≥19 DIV), the level of depolarization of mitochondrial membrane was also found to be increased above diploid neurons for all glutamate concentrations >25 μM. There were also significant differences in the kinetics of the Rh123 signal between diploid and Ts16 neurons. Generally the rise time and recovery of Rh123 signal increased with the applied glutamate concentration. The rise time and recovery of depolarization were larger in Ts16 neurons as compared with diploid neurons. The difference in the time to the maximum of the Rh123 signal became significant at concentrations ≥0.5 mM glutamate in all age groups. The recovery of mitochondrial membrane potential was significantly prolonged only in concentrations ≤100 μM glutamate, and this difference was particularly obvious in age groups II and III (Table 3).

Glutamate induces changes in NAD(P)H/NAD(P)$^+$ ratio in diploid and Ts16 neurons

Increases in $[Ca^{2+}]_i$ may lead to intramitochondrial Ca^{2+} accumulation, which in turn may increase respiration via activation of different intramitochondrial enzymes of the citrate cycle, namely pyruvate dehydrogenase, NAD^+-isocitrate dehydrogenase, and α-ketoglutarate dehydrogenase (Moreno-Sánchez and Hansford, 1988; Richter and Kass, 1991). Increased activity of the citrate cycle results in an increase in the NADH/NAD^+ ratio (Duchen et al., 1993). We therefore measured the autofluorescence that is mediated by the NAD(P)H fraction. The autofluorescence signal measured under these conditions is derived from both mitochondrial and cytosolic NADH and NADPH. Because the autofluorescence spectra overlap, it is not possible to differentiate between the signals originating from these two; for this reason we refer to NAD(P)H, indicating that the signals are derived from either NADH or NADPH or both. Under these conditions, an increase in autofluorescence signal indicates an increase in the reduced state of the pyridine nucleotide, i.e., NAD(P)H, and a decrease in autofluorescence signal indicates an increased oxidation to NAD(P)$^+$.

Figure 8 represents changes in NAD(P)H autofluorescence induced by application of 100 μM glutamate in all age groups for diploid and Ts16 neurons ($n \geq 9$ out of four different cultures for

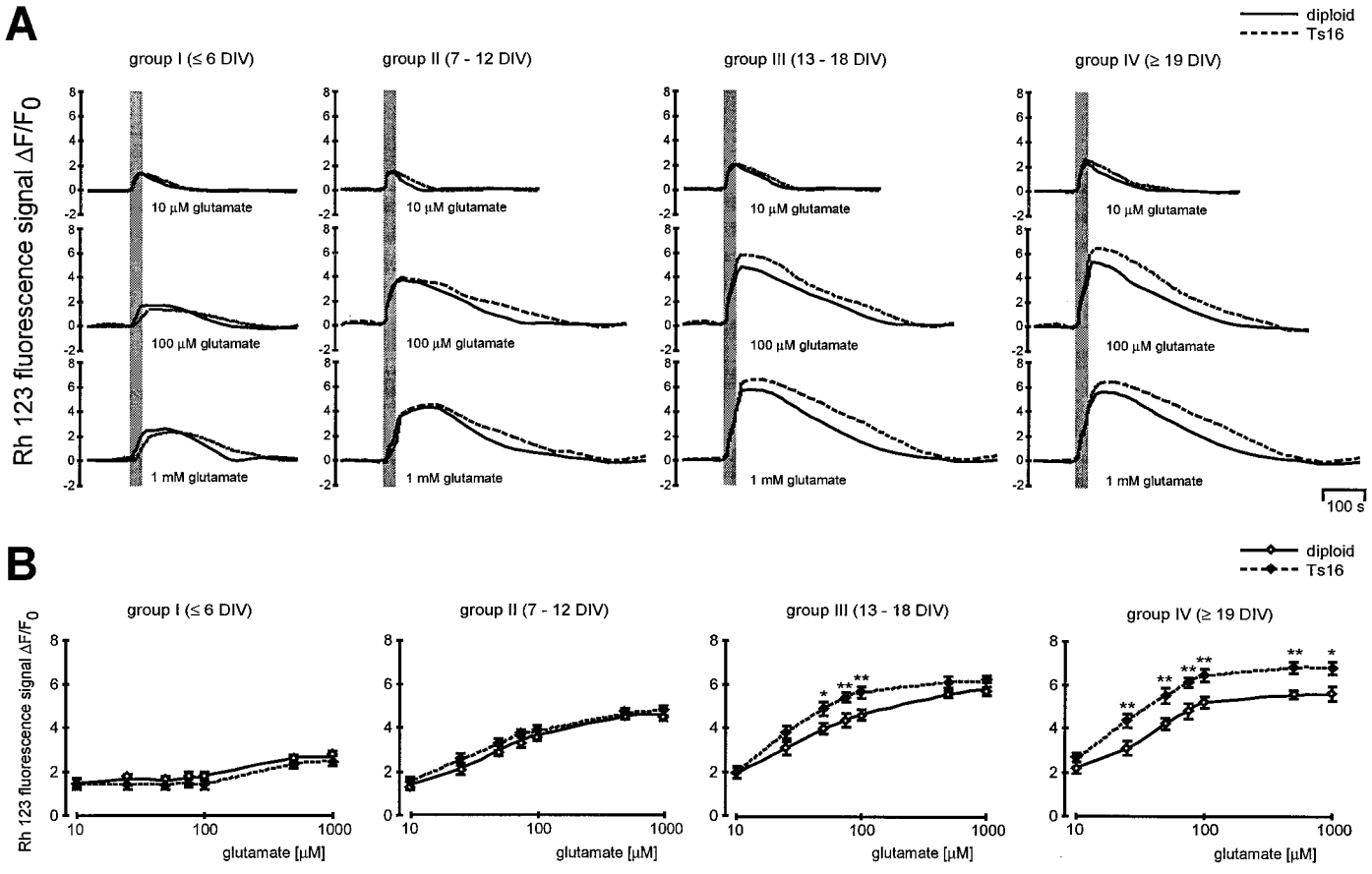

Figure 7. Depolarization of mitochondrial membrane after glutamate stimulation. *A*, Depolarization of mitochondrial membrane caused by glutamate stimulation for diploid (*solid lines*) and Ts16 (*dashed lines*) neurons. For stimulation, cultures were exposed to different concentrations of glutamate for 30 sec. The plots are based on the means of 24–36 neurons out of three experiments for each age group. Ts16 neurons showed a retardation in recovery of mitochondrial membrane potential compared with diploid neurons for all age groups and at all tested glutamate concentrations. *B*, Maximum Rh123 fluorescence signal as a function of glutamate concentration (logarithmic scale). Except for the youngest age group (≤ 6 DIV), Ts16 neurons were characterized by a larger rise in the Rh123 signal. After 2 weeks in culture, Ts16 neurons showed a significantly larger rise in Rh123 signal for 50–100 μM glutamate compared with diploid neurons. After 3 weeks in culture, the rise in Rh123 signal was significant for glutamate concentrations ≥ 25 μM (*$p < 0.05$; **$p < 0.01$).

Table 2. Depolarization of mitochondrial membrane after glutamate stimulation

	Diploid				Ts16			
Glutamate concentration (nM)	Group I (≤6 DIV)	Group II (7–12 DIV)	Group III (13–18 DIV)	Group IV (≥19 DIV)	Group I (≤6 DIV)	Group II (7–12 DIV)	Group III (13–18 DIV)	Group IV (≥19 DIV)
10	1.41 ± 0.20	1.29 ± 0.22	1.95 ± 0.25	2.20 ± 0.27	1.35 ± 0.22	1.39 ± 0.24	1.97 ± 0.27	2.55 ± 0.30
25	1.58 ± 0.24	1.98 ± 0.27	3.08 ± 0.30	3.08 ± 0.33	1.38 ± 0.23	2.37 ± 0.26	3.80 ± 0.29	4.35 ± 0.32**
50	1.52 ± 0.20	2.77 ± 0.22	3.97 ± 0.25	4.22 ± 0.27	1.38 ± 0.25	3.03 ± 0.28	4.90 ± 0.31*	5.49 ± 0.34**
75	1.63 ± 0.25	3.20 ± 0.29	4.34 ± 0.32	4.80 ± 0.35	1.41 ± 0.17	3.52 ± 0.19	5.41 ± 0.21**	6.11 ± 0.23**
100	1.72 ± 0.19	3.44 ± 0.22	4.61 ± 0.24	5.20 ± 0.27	1.36 ± 0.21	3.62 ± 0.23	5.62 ± 0.26**	6.43 ± 0.28**
500	2.49 ± 0.14	4.26 ± 0.15	5.56 ± 0.17	5.56 ± 0.19	2.26 ± 0.20	4.40 ± 0.22	6.11 ± 0.24	6.80 ± 0.27**
1000	2.57 ± 0.24	4.34 ± 0.27	5.80 ± 0.30	5.60 ± 0.33	2.37 ± 0.21	4.53 ± 0.23	6.16 ± 0.26	6.80 ± 0.28*

After incubation with Rh123 (10 μg/ml), diploid and Ts16 hippocampal cultures of all age groups were stimulated with glutamate for 30 sec. In the table, the maximum Rh123 increase, given in $\Delta F/F_0$, indicates the amount of mitochondrial membrane depolarization after glutamate-induced $[Ca^{2+}]_i$ increase. The data represent results with glutamate concentrations between 10 nM and 1 mM for all age groups out of three different preparations. Asterisks represent statistical significance between diploid and Ts16 data within each age group (*$p < 0.05$; **$p < 0.01$).

both diploid and Ts16 neurons). Single characteristic recordings are shown. The glutamate stimulus of 30 sec induced an immediate decrease of NAD(P)H autofluorescence signal in both diploid and Ts16 neurons. The amount of NAD(P)H decline showed no significant difference between diploid and Ts16 neurons (Fig. 8*C*). However, in contrast to diploid neurons, Ts16 neurons displayed a prolonged recovery. The duration of NAD(P)H signal recovery increased with age in culture. Ts16 neurons of age groups II, III, and IV (≥7 DIV) required a significantly longer time for recovery to baseline than diploid neurons (II: diploid

Table 3. Kinetics of glutamate-induced depolarization and after repolarization of mitochondrial membrane in diploid and Ts16 neurons

	Diploid				Ts16			
	Group I (≤6 DIV)	Group II (7–12 DIV)	Group III (13–18 DIV)	Group IV (≥19 DIV)	Group I (≤6 DIV)	Group II (7–12 DIV)	Group III (13–18 DIV)	Group IV (≥19 DIV)
A. Glutamate concentration (nM)								
10	30 ± 13	20 ± 13	15 ± 14	20 ± 14	30 ± 15	25 ± 14	25 ± 14	30 ± 15
100	50 ± 7	45 ± 7	50 ± 8	40 ± 8	62 ± 8	50 ± 9	50 ± 9	55 ± 9
1000	90 ± 6	85 ± 6	71 ± 6	55 ± 6	130 ± 7***	133 ± 7***	116 ± 7***	116 ± 7***
B. Glutamate concentration (nM)								
10	110 ± 40	85 ± 53	85 ± 52	157 ± 60	120 ± 42	180 ± 68**	130 ± 62*	230 ± 74
100	220 ± 24	264 ± 33	287 ± 27	374 ± 36	300 ± 22*	414 ± 42**	388 ± 39**	455 ± 41
1000	441 ± 21	475 ± 27	457 ± 32	495 ± 28	500 ± 19	560 ± 35	515 ± 31	551 ± 33

A, Data represent the time to maximum (in seconds) of Rh123 signal after application of 10 μM, 100 μM, and 1 mM glutamate for 30 sec. In contrast to diploid neurons in all age groups, Ts16 neurons stimulated with 1 mM glutamate showed a significantly slower Rh123 rise time to maximum. For concentrations ≤100 μM glutamate, no significant differences were observed in Rh123 rise times between diploid and Ts16 neurons.

B, Recovery time (in seconds) of Rh123 signal-to-basal level indicates the time for repolarization of mitochondrial membrane. The recovery of Rh123 signal was significantly slower for concentrations ≤100 μM, especially in age groups II and III. Stimulation with 1 mM glutamate resulted in a slightly slower but not significant recovery of Rh123 signal. Asterisks represent statistical significance between diploid and Ts16 data within each age group (*$p < 0.05$; **$p < 0.01$; ***$p < 0.001$).

190 ± 58 sec, Ts16 1090 ± 239 sec, $p < 0.001$; III: diploid 158 ± 48 sec, Ts16 853 ± 193 sec, $p < 0.001$; IV: diploid 340 ± 64 sec, Ts16 1768 ± 238 sec, $p < 0.001$) (Fig. 8*D*). In diploid neurons, an overshooting response with an increase in the NAD(P)H signal was noted, pointing to a secondary Ca^{2+} or glutamate-dependent stimulation of the citrate cycle. This overshooting response was dependent on age in culture in both amplitude of NAD(P)H autofluorescence increase and rise time to peak. Except for the youngest age group, such overshooting responses were not observed in Ts16 cultures, suggesting a reduction or loss of compensatory citrate cycle activation (Fig. 8*E,F*).

Effects of cyclosporin A on glutamate-induced changes in NAD(P)H/NAD(P)$^+$ ratio

Depolarization of mitochondrial membranes after glutamate-induced rises in $[Ca^{2+}]_i$ and Ca^{2+} accumulation in mitochondria may result in the opening of permeability transition pores. Mitochondrial membrane permeability transition is thought to mediate oxidative damage to mitochondria and therefore induce neuronal cell death (Takeyama et al., 1993; Ankarcrona et al., 1996; Schinder et al., 1996). The immunosuppressant drug cyclosporin A has been demonstrated to inhibit the nonspecific mitochondrial permeability transition (Broekemeier et al., 1992; Kass et al., 1992). Therefore we used cyclosporin A to investigate the role of mitochondrial membrane permeability transition for the glutamate-induced reduction in NAD(P)H autofluorescence signal in Ts16 neurons in comparison to diploid neurons.

Figure 9*A* shows that in the presence of 1.5 μM cyclosporin A, no NAD(P)H decrease was observed in either diploid or Ts16 neurons in response to 100 μM glutamate. Instead, an initially slow and finally rapid increase in NAD(P)H autofluorescence signal was measured. In the presence of cyclosporin A, the maximum level and duration of the glutamate-induced rise in NAD(P)H signal were elevated. Furthermore, we observed no significant age dependence in NAD(P)H signal response to glutamate except for age group I (≤6 DIV). This supports the idea that a $[Ca^{2+}]_i$ increase is required to change the NAD(P)H signal in the presence or absence of cyclosporin A. In Ts16 neurons (age group II–IV), however, the NAD(P)H maxima was reduced by ~15% in comparison with diploid neurons (Fig. 9*B*). Moreover, Ts16 neurons showed a significant delay in NAD(P)H signal increase (mean time to maximum for age group II–IV: diploid 153 ± 21 sec, Ts16 262 ± 26 sec; $p < 0.001$ for each age group, diploid vs Ts16 neurons) (Fig. 9*C*). The findings imply that mitochondrial permeability transition may be involved in the absence of the NAD(P)H signal overshoot after application of glutamate in Ts16 neurons.

DISCUSSION

The present study demonstrates the important role of changes in calcium homeostasis and mitochondrial function in neuronal cell loss occurring in hippocampal cell cultures from Ts16 mice. In particular, our study describes alterations in the NAD(P)H autofluorescence signal, which served as a marker of mitochondrial energy metabolism. A connection between disturbances of intracellular Ca^{2+} regulation, mitochondrial dysfunction, and neuronal cell death in Ts16 cultures is suggested.

Survival of diploid and Ts16 hippocampal neurons in culture

Ts16 neurons display a significantly increased death rate in comparison to diploid control neurons under culture conditions. Glutamate receptor antagonists APV and NBQX as well as cyclosporin A, an inhibitor of the mitochondrial permeability transition, had only minor effects on the observed death rate in diploid and Ts16 cultures. In contrast, tocopherol (vitamin E) protected Ts16 cultures against the augmented neuronal loss. The neuroprotective effect from the membrane-localized antioxidant tocopherol indicates an elevated concentration of reactive oxygen species (ROS) in Ts16 cultures. An increased generation of ROS in cortical neurons from fetal Down's individuals has been suggested to cause neuronal apoptosis *in vitro* (Busciglio and Yankner, 1995). Increased ROS levels in culture may result from increased production or a reduced disposal of ROS molecules or both. Several investigators have proposed that the triplication of Cu/Zn-SOD in Ts16 mice and Down's individuals results in an elevated level of ROS (Sinet, 1982; Groner et al., 1994; Bar-Peled et al., 1996; Peled-Kamar et al., 1997). Furthermore, in transgenic mice with an elevated level of Cu/Zn-SOD, a disruption in cellular ROS metabolism has been demonstrated (Avraham et al., 1988, 1991; Peled-Kamar et al., 1995; Lotem et al., 1996). This finding may result from the capability of Cu/Zn-SOD to catalyze the formation of ROS using anionic scavengers and H_2O_2 as substrates (Yim et al., 1993). In Ts16 cultures, an increased

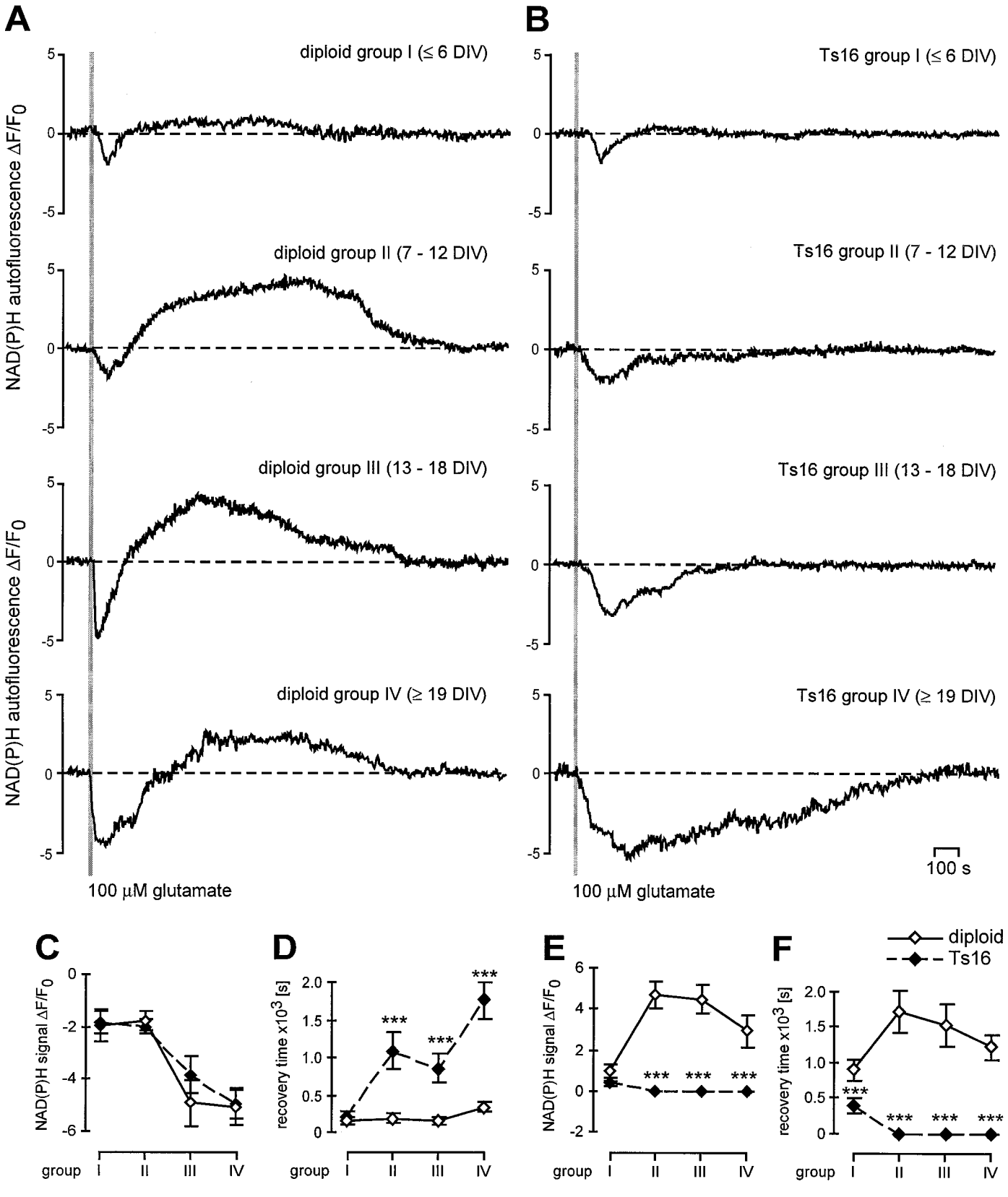

Figure 8. Changes in NAD(P)H autofluorescence after glutamate stimulation. *A, B*, Cultures of the different age groups were superfused with ACSF, and the NAD(P)H autofluorescence signal was directly measured from clusters consisting of 10–15 optically identified neurons. For stimulation, cells were exposed to 100 μM glutamate for 10 sec. The representative plots show the typical response for diploid (*A*) and Ts16 (*B*) neurons ($n \geq 9$ out of 4 different cultures) after glutamate stimulation. As Ca^{2+} enters the neuron, the mitochondria depolarize, and, as a consequence, the respiratory chain activity increases to restore the mitochondrial membrane potential. This increased respiratory activity will lead to an increased *(Figure legend continues)*

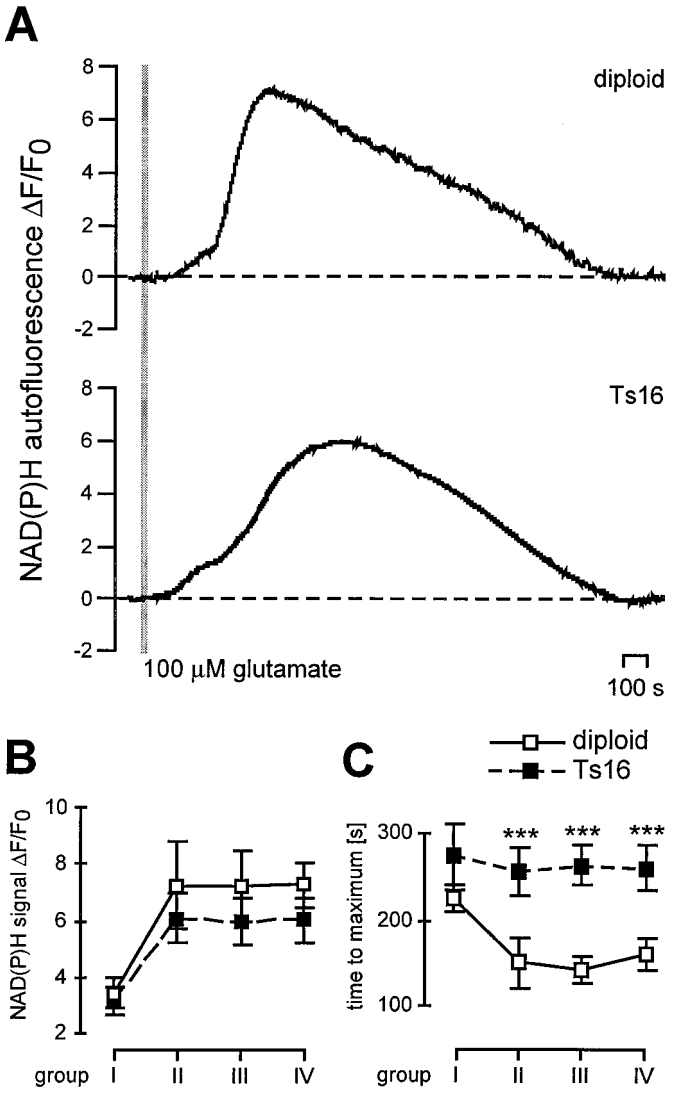

Figure 9. Glutamate-induced change in the NAD(P)H signal in the presence of cyclosporin A. *A*, The represented plots show the typical response for diploid (*top*) and Ts16 (*bottom*) neurons ($n = 9$ out of 3 different cultures) on stimulation with 100 μM glutamate for 10 sec. In contrast to the absence of cyclosporin A, no NAD(P)H signal decrease was observed in either diploid or Ts16 neurons. The overshoot in NAD(P)H signal is characterized by an initially slow, and finally rapid, rise. Note the increased decay and reduced rise in NAD(P)H signal in Ts16 neurons in comparison to diploid neurons. *B*, Maximum NAD(P)H signal increase in the presence of 1.5 μM cyclosporin A after the application of 100 μM glutamate for 10 sec in diploid (*open squares, solid line*) and Ts16 (*closed squares, dashed line*) neurons. Except for the youngest age group (≤6 DIV), diploid neurons showed an increased NAD(P)H signal maximum in comparison with Ts16 neurons. *C*, Rise time to NAD(P)H signal maximum was significant increased in Ts16 neurons of age groups II, III, and IV (Ts16 vs diploid, *** $p < 0.001$).

production of superoxide radicals by microglial cells has been shown (Colton et al., 1990). Furthermore, the observation that cultured Ts16 neurons possess a significantly reduced level of the intracellular ROS-scavenger glutathione in comparison to diploid neurons (Stabel-Burow et al., 1997) also points to elevated levels of ROS.

Age-dependent changes in basal $[Ca^{2+}]_i$ in Ts16 neurons

Neuronal Ca^{2+} homeostasis is regulated by Ca^{2+} influx through voltage-activated and receptor-gated Ca^{2+} channels and Ca^{2+} efflux via the Na^+/Ca^{2+} exchanger and ATP-dependent Ca^{2+} pumps. Furthermore, $[Ca^{2+}]_i$ is buffered by ATP-dependent

←

formation of ROS because ~1–2% of the oxygen consumed during respiration is transformed into ROS by the mitochondrial respiratory chain (Poyton and McEwen, 1996). The brief decrease in NAD(P)H fluorescence from diploid neurons correlates well with this assumption. It may well be that a larger production of ROS in Ts16 neurons caused by the prolonged mitochondrial membrane depolarization causes an augmented decrease in NAD(P)H autofluorescence signal. As a consequence, the Ca^{2+}-dependent changes in enzyme activity may be hidden and terminated by the time that the NAD(P)H signal has finally recovered to baseline. *C*, The amount of decrease in NAD(P)H fluorescence signal was age dependent for both diploid (*open squares, solid line*) and Ts16 (*closed squares, dashed line*) neurons. *D*, Recovery time after glutamate-induced NAD(P)H decrease for diploid and Ts16 neurons. Ts16 neurons showed an age-dependent rise in the recovery time of NAD(P)H fluorescence signal in comparison with diploid neurons (*** $p < 0.001$). *E*, Maximum peak of NAD(P)H fluorescence signal overshoot after glutamate application for all age groups in diploid and Ts16 neurons. Except for the youngest age group (≤6 DIV), Ts16 neurons were lacking in NAD(P)H fluorescence signal overshoot (Ts16 vs diploid, *** $p < 0.001$). The maximum peak of NAD(P)H fluorescence signal overshoot observed in diploid neurons after glutamate stimulation increased to a maximum after 1 week in culture. Older diploid age groups showed a reduction in the maximum peak of NAD(P)H fluorescence signal overshoot. *F*, Recovery time of NAD(P)H fluorescence signal overshoot was measured between the maximum peak of the NAD(P)H signal and the first time the NAD(P)H signal returned to the basal NAD(P)H value. The recovery time of NAD(P)H signal overshoot showed a maximum for diploid neurons out of age group II, similar to the maximum peak of the NAD(P)H signal overshoot shown in *E*.

Ca^{2+} transport into intracellular stores and binding to intracellular proteins (for review, see Carafoli, 1987). We have not yet studied the mechanisms underlying the age-dependent basal $[Ca^{2+}]_i$ increase in Ts16 neurons that we have described in this study. Changes in electrical properties in cultured hippocampal Ts16 neurons have been reported (Galdzicki et al., 1993). Ts16 neurons show an abnormal action potential and an increased plasma membrane Ca^{2+} conductance (Rapoport and Galdzicki, 1994). Ca^{2+} shift into mitochondria has been shown as an important part of intracellular Ca^{2+} regulation (Gunter et al., 1994; White and Reynolds, 1995). A reduced buffering capacity or elevated mitochondrial Ca^{2+} release may result in the observed $[Ca^{2+}]_i$ increase in Ts16 neurons. Such mitochondrial Ca^{2+} dysregulation has been reported to be caused by an elevated ROS concentration in Ts16 neurons (Weis et al., 1994).

Previous studies have shown an abnormal calcium homeostasis in astrocytes from Ts16 cultures (Bambrick et al., 1997; Müller et al., 1997). Thus the average basal $[Ca^{2+}]_i$ in Ts16 astrocytes was more than twice as high as in diploid astrocytes. Furthermore, elevated amounts of calcium were observed in endoplasmatic reticulum Ca^{2+} stores in Ts16 astrocytes that may result from increased intracellular Ca^{2+} load or augmented mitochondrial Ca^{2+} efflux (Bambrick et al., 1997).

An interesting possibility is a destabilized calcium homeostasis attributable to the overexpression of βAPP as reported by Mattson and colleagues (1993a), which is of particular interest in view of the fact that βAPP is overexpressed in Ts16 mice. It has been shown that βAPP expression is regulated by development (Holtzman et al., 1992). Therefore, changes in the expression of βAPP during neuronal development may result in the significantly increased basal $[Ca^{2+}]_i$ in Ts16. To our knowledge there are no data available that describe an effect of βAPP on basal $[Ca^{2+}]_i$.

Considering that Ca^{2+}-dependent elevation in neuronal death is reported when $[Ca^{2+}]_i$ rises above 300 nM for longer times (Johnson et al., 1992), we assume that increases in basal $[Ca^{2+}]_i$ do not contribute directly to the increased death rate in Ts16 neurons.

Glutamate-induced changes of the neuronal death rate

Neuronal survival decreased drastically after application of glutamate in both diploid and Ts16 cultures. Glutamate-induced neurotoxicity is expected to occur gradually and to be triggered by a rapid increase in $[Ca^{2+}]_i$ via NMDA receptors (Choi, 1988a, 1992, 1995). Thus, selective inhibition of NMDA receptors or absence of extracellular Ca^{2+} is known to protect neurons against glutamate-effected elevation in cell death (Choi, 1988b; Tymianski et al., 1993). This is in line with the current findings, where a reduction in neuronal death was observed after glutamate application in the absence of extracellular Ca^{2+} or in the presence of the NMDA antagonist APV in diploid and Ts16 cultures. In previous studies it has been shown that glutamate application induced large increases in $[Ca^{2+}]_i$, leading to a depolarization of mitochondrial membrane (Duchen et al., 1993; Hartley et al., 1993; Schinder et al., 1996). Both elevation in $[Ca^{2+}]_i$ and depolarization of mitochondrial membrane are thought to induce opening of mitochondrial permeability transition pores (Hoek et al., 1995; Bernardi, 1996). The mitochondrial permeability transition leads to mitochondrial swelling, collapse of mitochondrial membrane potential, and uncoupling of oxidative phosphorylation (Broekemeier et al., 1992; Zazueta et al., 1994; Bernardi, 1996). It is of particular interest that a blocking of the mitochondrial permeability transition using cyclosporin A prevented glutamate-induced Ca^{2+}-mediated neurotoxicity in both diploid and Ts16 cultures. The reduced neuronal cell loss in the presence of cyclosporin A indicates a key role of mitochondria in glutamate-induced elevated exitotoxicity, as suggested previously by several investigators (Bernardi, 1992; Reed and Savage, 1995; Schinder et al., 1996; Waring and Beaver, 1996; Zamzami et al., 1996).

Glutamate causes augmented neuronal cell death in Ts16 cultures

The results presented in this study show that glutamate caused an elevated neuronal death rate in Ts16 cultures in comparison with diploid cultures. We propose that disturbances in the interplay between Ca^{2+} homeostasis and mitochondrial function triggers the augmented neuronal death in Ts16 cultures. Furthermore, enhanced ROS generation in Ts16 cultures may contribute to the damaging neuronal cascade.

In Ts16 neurons, $[Ca^{2+}]_i$ increases induced by either K^+ or glutamate application displayed a prolonged recovery and an elevated Ca^{2+} integral. As a consequence, we postulated a delayed repolarization of mitochondrial membranes after the prolonged increases in $[Ca^{2+}]_i$ in Ts16 neurons. Indeed we found that depolarizations of mitochondrial membranes recovered more slowly in Ts16 than in diploid neurons. Elevated $[Ca^{2+}]_i$ may be responsible for mitochondrial membrane potential disturbance (Gunter et al., 1994) and mitochondrial damage (Mattson et al., 1993c), and we found that Ca^{2+}-induced depolarizations of mitochondrial membranes were not only prolonged but also increased in Ts16 neurons in comparison to diploid neurons. In addition to alterations in Ca^{2+} homeostasis, other factors may contribute to this increased depolarization and prolonged recovery of the mitochondrial membrane. ROS molecules are important candidates. Several studies have shown that glutamate causes an increase in ROS formation (Dugan et al., 1995; Reynolds and Hastings, 1995). Elevated ROS concentration is expected to increase direct NADH oxidation (Bandy and Davison, 1990; Duchen et al., 1993). Therefore, the prolonged initial reduction of NAD(P)H signal and the absence of the NAD(P)H signal overshoot that followed the application of glutamate in Ts16 neurons may indicate an elevated ROS generation. This suggestion is supported by the observed NAD(P)H signal overshoot that corresponds to the stimulation of mitochondrial Ca^{2+}-dependent dehydrogenases in Ts16 neurons during blockade of mitochondrial permeability transition by cyclosporin A. This mitochondrial permeability transition is induced by Ca^{2+} in conjunction with other agents, particularly ROS (Gunter and Pfeiffer, 1990; Gunter et al., 1994; Hoek et al., 1995). Furthermore, Kowaltowski and colleagues (1996) showed that the mitochondrial permeability transition in the presence of Ca^{2+} is dependent on mitochondrial-generated reactive oxygen species. Thus an increased concentration of ROS may be involved in this mechanism and may amplify the Ca^{2+}-induced mitochondrial permeability transition (Takeyama et al., 1993; Weis et al., 1994; Richter et al., 1995). Moreover, cyclosporin A has been reported to prevent further mitochondrial ROS production (Kass et al., 1992; Bernardi, 1996; Costantini et al., 1996).

Several findings may indicate a generally increased ROS generation in Ts16 neurons (Fig. 10): (1) reduced neuronal death rate in the presence of tocopherol, (2) prolonged reduction in NAD(P)H autofluorescence signal after depolarization of the mitochondrial membrane, (3) a Ca^{2+}-induced NAD(P)H signal overshoot in the presence of cyclosporin A, and (4) reduced

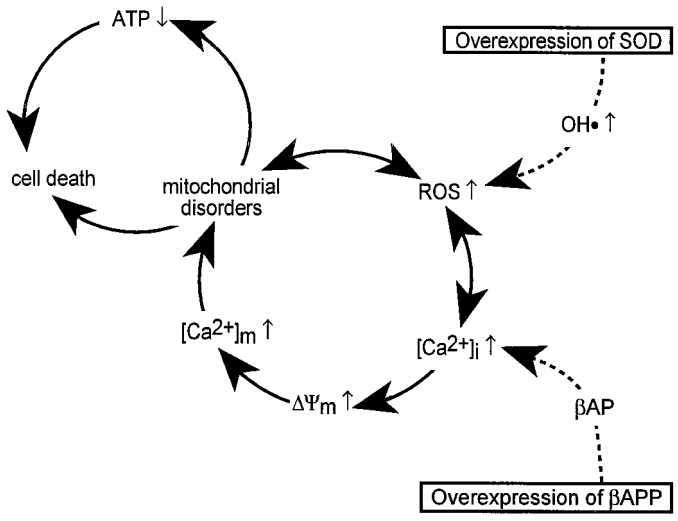

Figure 10. Schematic representation of potential pathways responsible for disturbed Ca^{2+} homeostasis, mitochondrial dysfunction, and increased neuronal cell death in Ts16 neurons. Neurons from Ts16 mice are characterized by an overexpression of βAPP and Cu/Zn-SOD. The βAPP product βAP is known to disturb Ca^{2+} homeostasis and elevate ROS concentration. Cu/Zn-SOD has been reported to catalyze the formation of ROS using anionic scavengers and H_2O_2 as substrates. Elevated ROS concentration is known to cause mitochondrial damage and mediate changes in Ca^{2+} homeostasis. As a consequence, the direct oxidation of NADH to NAD^+ will be elevated. Therefore, the electron supply out of the citrate cycle via NADH to the mitochondrial respiratory chain and mitochondrial proton pumps will be disturbed. Furthermore, mitochondria are thought to be the major buffering compartments for elevation of $[Ca^{2+}]_i$ after brief applications of glutamate. Mitochondrial Ca^{2+} overload-induced Ca^{2+} cycling across the inner mitochondrial membrane, i.e., continuous Ca^{2+} release and uptake, is known to damage mitochondria. This leads to a depolarization of the mitochondrial membrane potential ($\Delta\Psi_m$) and an uncoupling of the mitochondrial electron transport chain and oxidative phosphorylation. This results in an impairment of ATP synthesis. The deficiency in ATP prevents the sufficient function of plasma membrane Ca^{2+} ATPase followed by a further elevation in cytosolic Ca^{2+} and causes cell death.

glutamate-induced neurotoxicity in the presence of cyclosporin A and, to some extent, in the presence of tocopherol. Furthermore, overexpression of Cu/Zn-SOD (Groner et al., 1994) and βAPP via the product βAP can cause an increased production of ROS (Behl et al., 1994). Elevated ROS concentration is known to cause mitochondrial damage (Beal et al., 1993; Dykens, 1994; Bolaños et al., 1995, 1997) and disturb Ca^{2+} homeostasis (Richter and Kass, 1991; Gunter et al., 1994; Mattson, 1994; Bondy, 1995; Mattson et al., 1995; White and Reynolds, 1996). Further studies on the Ts16 mouse model are needed to determine whether the primary defect is linked to Ca^{2+} homeostasis or mitochondrial ROS production.

REFERENCES

Ankarcrona M, Dypbukt JM, Orrenius S, Nicotera P (1996) Calcineurin and mitochondrial function in glutamate-induced neuronal cell death. FEBS Lett 394:321–324.

Aubin JE (1979) Autofluorescence of viable cultured mammalian cells. J Histochem Cytochem 27:36–43.

Ault B, Caviedes P, Hidalgo J, Epstein CJ, Rapoport SI (1989) Electrophysiological analysis of cultured fetal mouse dorsal root ganglion neurons transgenic for human superoxide dismutase-1, a gene in the Down syndrome region of chromosome 21. Brain Res 497:191–194.

Avraham KB, Schickler M, Sapoznikov D, Yarom R, Groner Y (1988) Down's syndrome: abnormal neuromuscular junction in tongue of transgenic mice with elevated levels of human Cu/Zn-superoxide dismutase. Cell 54:823–829.

Avraham KB, Sugarman H, Rotshenker S, Groner Y (1991) Down's syndrome: morphological remodelling and increased complexity in the neuromuscular junction of transgenic CuZn-superoxide dismutase mice. J Neurocytol 20:208–215.

Aw TY, Andersson BS, Jones DP (1987) Mitochondrial transmembrane ion distribution during anoxia. Am J Physiol 252:C356–C361.

Bambrick LL, Yarowsky PJ, Krueger BK (1995) Glutamate as a hippocampal neuron survival factor: an inherited defect in the trisomy 16 mouse. Proc Natl Acad Sci USA 92:9692–9696.

Bambrick LL, Golovina VA, Blaustein MP, Yarowsky PJ, Krueger BK (1997) Abnormal calcium homeostasis in astrocytes from trisomy 16 mouse. Glia 19:352–358.

Bandy B, Davison AJ (1990) Mitochondrial mutations may increase oxidative stress: implications for carcinogenesis and aging? Free Radical Biol Med 8:523–539.

Banker GA, Cowan WM (1977) Rat hippocampal neurons in dispersed cell culture. Brain Res 126:397–425.

Bar-Peled O, Korkotian E, Segal M, Groner Y (1996) Constitutive overexpression of Cu/Zn superoxide dismutase exacerbates kainic acid-induced apoptosis of transgenic-Cu/Zn superoxide dismutase neurons. Proc Natl Acad Sci USA 93:8530–8535.

Beal MF, Hyman BT, Koroshetz W (1993) Do defects in mitochondrial energy metabolism underlie the pathology of neurodegenerative diseases? Trends Neurosci 16:125–131.

Behl C, Davis JB, Lesley R, Schubert D (1994) Hydrogen peroxide mediates amyloid β protein toxicity. Cell 77:817–827.

Bernardi P (1992) Modulation of the mitochondrial cyclosporin A-sensitive permeability transition pore by the proton electrochemical gradient. J Biol Chem 267:8834–8839.

Bernardi P (1996) The permeability transition pore. Control points of cyclosporin A-sensitive mitochondrial channel involved in cell death. Biochim Biophys Acta 1275:5–9.

Bleakman D, Roback JD, Wainer BH, Miller RJ, Harrison NJ (1993) Calcium homeostasis in rat septal neurons in tissue culture. Brain Res 600:257–267.

Bolaños JP, Heales SJR, Land JM, Clark JB (1995) Effect of peroxynitrite on the mitochondrial respiratory chain: differential susceptibility of neurones and astrocytes in primary culture. J Neurochem 64:1965–1972.

Bolaños JP, Almeida A, Stewart V, Peuchen S, Land JM, Clark JB, Heales SJR (1997) Nitric oxide-mediated mitochondrial damage in the brain: mechanisms and implications for neurodegenerative diseases. J Neurochem 68:2227–2240.

Bondy SC (1995) The relation of oxidative stress and hyperexcitation to neuronal disease. Proc Soc Exp Biol Med 208:337–345.

Broekemeier KM, Carpenter-Deyo L, Reed DJ, Pfeiffer DR (1992) Cyclosporin A protects hepatocytes subjected to high Ca^{2+} and oxidative stress. FEBS Lett 304:192–194.

Busciglio J, Yankner BA (1995) Apoptosis and increased generation of reactive oxygen species in Down's syndrome neurons in vitro. Nature 378:776–779.

Carafoli E (1987) Intracellular calcium homeostasis. Annu Rev Biochem 56:395–433.

Chen LB (1989) Fluorescent labeling of mitochondria. In: Methods in cell biology, Vol 29, Part A, Fluorescence microscopy of living cells in culture (Taylor DL, Wang Y-L, eds), pp 103–123. San Diego: Academic.

Choi DW (1988a) Calcium-mediated neurotoxicity: relationship to specific channel types and role in ischemic damage. Trends Neurosci 11:465–469.

Choi DW (1988b) Glutamate neurotoxicity and diseases of the nervous system. Neuron 1:623–634.

Choi DW (1992) Excitotoxic cell death. J Neurobiol 23:1261–1276.

Choi DW (1995) Calcium: still center-stage in hypoxic-ischemic neuronal death. Trends Neurosci 18:58–60.

Colton CA, Yao J, Gilbert D, Oster-Granite ML (1990) Enhanced production of superoxide anion by microglia from trisomy 16 mice. Brain Res 519:236–242.

Costantini P, Chernyak BV, Petronilli V, Bernardi P (1996) Modulation of the mitochondrial permeability transition pore by pyridine nucleotides and dithiol oxidation at two separate sites. J Biol Chem 271:6746–6751.

Coyle JT, Oster-Granite ML, Reeves RH, Gearhart J (1988) Down

syndrome, Alzheimer's disease and the trisomy 16 mouse. Trends Neurosci 11:390–394.
Dubinsky JM, Kristal BS, Elizondo-Fournier M (1995) On the probabilistic nature of excitotoxic neuronal death in hippocampal neurons. Neuropharmacology 34:701–711.
Duchen MR (1992a) Fluorescence: monitoring cell chemistry in vivo. In: Monitoring neuronal activity. A practical approach (Stamford JA, ed), pp 231–260. New York: IRL.
Duchen MR (1992b) Ca^{2+}-dependent changes in the mitochondrial energetics in single dissociated mouse sensory neurons. Biochem J 283:41–50.
Duchen MR, Biscoe TJ (1992) Relative mitochondrial membrane potential and $[Ca^{2+}]_i$ in type 1 cells isolated from rabbit carotid body. J Physiol (Lond) 450:33–61.
Duchen MR, Smith PA, Ashcroft FM (1993) Substrate-dependent changes in mitochondrial function, intracellular free calcium concentration and membrane channels in pancreatic β-cells. Biochem J 294:35–42.
Dugan LL, Sensi SL, Canzoniero LMT, Handran SD, Rothman SM, Lin T-S, Goldberg MP, Choi DW (1995) Mitochondrial production of reactive oxygen species in cortical neurons following exposure to *N*-methyl-D-aspartate. J Neurosci 15:6377–6388.
Dykens JA (1994) Isolated cerebral and cerebellar mitochondria produce free radicals when exposed to elevated Ca^{2+} and Na^{+}: implications for neurodegeneration. J Neurochem 63:584–591.
Emaus RK, Grunwald R, Lemasters JJ (1986) Rhodamine 123 as a probe of transmembrane potential in isolated rat-liver mitochondria: spectral and metabolic properties. Biochim Biophys Acta 850:436–448.
Epstein CJ (1986) The neurobiology of Down syndrome. New York: Raven.
Galdzicki Z, Coan E, Rapoport SI (1993) Cultured hippocampal neurons from trisomy 16 mouse, a model for Down syndrome, have abnormal action potential due to reduced inward sodium current. Brain Res 604:69–78.
Groner Y, Elroy-Stein O, Avraham KB, Schickler M, Knobler H, Minc-Golomb D, Bar-Peled O, Yarom R, Rotshenker S (1994) Cell damage by excess CuZnSOD and Down's syndrome. Biomed Pharmacother 48:231–240.
Gropp A, Kolbus U, Giers D (1975) Systematic approach to the study of trisomy in the mouse. II. Cytogenet Cell Genet 14:42–62.
Grynkiewicz G, Poenie M, Tsien RY (1985) A new generation of calcium indicators with greatly improved fluorescence properties. J Biol Chem 260:3440–3450.
Gunter TE, Pfeiffer DR (1990) Mechanisms by which mitochondria transport calcium. Am J Physiol 258:C755–C786.
Gunter TE, Gunter KK, Sheu S-S, Gavin CE (1994) Mitochondrial calcium transport: physiological and pathological relevance. Am J Physiol 267:C313–C339.
Hansford RG (1980) Control of mitochondrial substrate oxidation. Curr Top Bioenerg 10:217–278.
Hansford RG (1985) Relation between mitochondrial calcium transport and control of energy metabolism. Rev Physiol Biochem Pharmacol 102:1–72.
Hartley DM, Kurth MC, Bjerkness L, Weiss JH, Choi DW (1993) Glutamate receptor-induced $^{45}Ca^{2+}$ accumulation in cortical cell culture correlates with subsequent neuronal degeneration. J Neurosci 13: 1993–2000.
Hoek JB, Farber JL, Thomas AP, Wang X (1995) Calcium ion-dependent signalling and mitochondrial dysfunction: mitochondrial calcium uptake during hormonal stimulation in intact liver cells and its implication for the mitochondrial permeability transition. Biochim Biophys Acta 1271:93–102.
Holtzman DM, Bayney RM, Li Y, Khosrovi H, Berger CN, Epstein CJ, Mobley WC (1992) Dysregulation of gene expression in mouse trisomy 16, an animal model of Down syndrome. EMBO J 11:619–627.
Johnson EM, Koike T, Franklin J (1992) A "calcium set-point hypothesis" of neuronal dependence on neurotrophic factor. Exp Neurol 115:163–166.
Johnson LV, Walsh ML, Chen LB (1980) Localization of mitochondria in living cells with rhodamine 123. Proc Natl Acad Sci USA 77:990–994.
Kass GEN, Juedes MJ, Orrenius S (1992) Cyclosporin A protects hepatocytes against prooxidant-induced cell killing. Biochem Pharmacol 44:1995–2003.
Kowaltowski AJ, Castilho RF, Vercesi AE (1996) Opening of the mitochondrial permeability transition pore by uncoupling or inorganic phosphate in the presence of Ca^{2+} is dependent on mitochondrial-generated reactive oxygen species. FEBS Lett 378:150–152.
Lane NJ, Balbo A, Rapoport SI (1996) A fine structural study of hippocampus and dorsal root ganglion in mouse trisomy 16, a model of Down's syndrome. Cell Biol Int 20:673–680.
Lotem J, Peled-Kamar M, Groner Y, Sachs L (1996) Cellular oxidative stress and the control of apoptosis by the wild-type p53, cytotoxic compounds, and cytokines. Proc Natl Acad Sci USA 93:9166–9171.
Mattson MP (1994) Calcium and neuronal injury in Alzheimer's disease. Ann NY Acad Sci 747:50–76.
Mattson MP, Kater SB (1988) Isolated hippocampal neurons in cyto-preserved long-term cultures: development of neuroarchitecture and sensitivity to NMDA. Int J Dev Neurosci 6:439–452.
Mattson MP, Kater SB (1989) Development and selective neurodegeneration in cell cultures from different hippocampal regions. Brain Res 490:110–125.
Mattson MP, Cheng B, Davis D, Bryant K, Lieberburg I, Rydel RE (1992) β-amyloid peptides destabilize calcium homeostasis and render human cortical neurons vulnerable to excitotoxicity. J Neurosci 12:376–389.
Mattson MP, Barger SW, Cheng B, Lieberburg I, Smith-Swintosky VL, Rydel RE (1993a) β-amyloid precursor protein metabolites and loss of neuronal Ca^{2+} homeostase in Alzheimer's disease. Trends Neurosci 16:409–414.
Mattson MP, Cheng B, Culwell AR, Esch FS, Lieberburg I, Rydel RE (1993b) Evidence for excitoprotective and intraneuronal calcium-regulating roles for secreted forms of the β-amyloid precursor protein. Neuron 10:243–254.
Mattson MP, Zhang Y, Bose S (1993c) Growth factors prevent mitochondrial dysfunction, loss of calcium homeostasis, and cell injury, but not ATP depletion in hippocampal neurons deprived of glucose. Exp Neurol 121:1–13.
Mattson MP, Barger SW, Begley JG, Mark RJ (1995) Calcium, free radicals, and excitotoxic neuronal cell death in primary cell culture. Methods Cell Biol 46:187–216.
Moreno-Sánchez R, Hansford RG (1988) Dependence of cardiac mitochondrial pyruvate dehydrogenase activity on intramitochondrial free Ca^{2+} concentration. Biochem J 256:403–412.
Müller W, Heinemann U, Schuchmann S (1997) Impaired Ca-signaling in astrocytes from the Ts16 mouse model of Down syndrome. Neurosci Lett 223:81–84.
Nicolli A, Basso E, Petronilli V, Wenger RM, Bernardi P (1996) Interactions of cyclophilin with the mitochondrial inner membrane and regulation of the permeability transition pore, a cyclosporin A-sensitive channel. J Biol Chem 271:2185–2192.
Nieminen A-L, Petrie TG, Lemasters JJ, Selman WR (1996) Cyclosporin A delays mitochondrial depolarization induced by *N*-methyl-D-aspartate in cortical neurons: evidence of the mitochondrial permeability transition. Neuroscience 75:993–997.
Orozco CB, Epstein CJ, Rapoport SI (1988) Voltage-activated sodium conductances in cultured normal and trisomy 16 dorsal root ganglion neurons from the fetal mouse. Dev Brain Res 38:265–274.
Oyama Y, Hayashi A, Ueha T, Maekawa K (1994) Characterization of 2′,7′-dichlorofluorescin fluorescence in dissociated mammalian brain neurons: estimation on intracellular content of hydrogen peroxide. Brain Res 635:113–117.
Pastorino JG, Snyder JW, Hoek JB, Farber JL (1995) Ca^{2+} depletion prevents anoxic death of hepatocytes by inhibiting mitochondrial permeability transition. Am J Physiol 268:C676–C685.
Peacock JH, Rush DF, Mathers LH (1979) Morphology of dissociated hippocampal cultures from fetal mice. Brain Res 196:231–246.
Peled-Kamar M, Lotem J, Okon E, Sachs L, Groner Y (1995) Thymic abnormalities and enhanced apoptosis of thymocytes and bone marrow cells in transgenic mice overexpressing Cu/Zn-superoxide dismutase: implications for Down syndrome. EMBO J 14:4985–4993.
Peled-Kamar M, Lotem J, Wirguin I, Weiner L, Hermalin A, Groner Y (1997) Oxidative stress mediates impairment of muscle function in transgenic mice with elevated level of wild-type Cu/Zn superoxide dismutase. Proc Natl Acad Sci USA 94:3883–3887.
Poyton RO, McEwen JE (1996) Crosstalk between nuclear and mitochondrial genomes. Annu Rev Biochem 65:563–607.
Rapoport SI, Galdzicki Z (1994) Electrical studies of cultured fetal human trisomy 21 and mouse trisomy 16 neurons identify functional

deficits that may lead to mental retardation in Down syndrome. Dev Brain Dysfunct 7:265–288.

Reed DJ, Savage MK (1995) Influence of metabolic inhibitors on mitochondrial permeability transition and glutathione status. Biochim Biophys Acta 1271:43–50.

Reynolds IJ, Hastings TG (1995) Glutamate induces the production of reactive oxygen species in cultured forebrain neurons following NMDA receptor activation. J Neurosci 15:3318–3327.

Richards SJ (1991) The neuropathology of Alzheimer's disease investigated by transplantation of mouse trisomy 16 hippocampal tissues. Trends Neurosci 14:334–338.

Richards SJ, Waters JJ, Beyreuther K, Masters CL, Wischik CM, Sparkman DR, White CL, Abraham CR, Dunnett SB (1991) Transplants of mouse trisomy 16 hippocampus provide a model of Alzheimer's disease neuropathology. EMBO J 10:297–303.

Richter C, Kass GEN (1991) Oxidative stress in mitochondria: its relationship to cellular Ca^{2+} homeostasis, cell death, proliferation, and differentiation. Chem Biol Interact 77:1–23.

Richter C, Gogvadze V, Laffranchi R, Schlapbach R, Schweizer M, Suter M, Walter P, Yaffee M (1995) Oxidants in mitochondria: from physiology to diseases. Biochim Biophys Acta 1271:67–74.

Rumble B, Retallack R, Hilbich C, Simms G, Multhaup G, Martins R, Hockey A, Montgomery P, Beyreuther K, Masters CL (1989) Amyloid A4 protein and its precursor in Down's syndrome and Alzheimer's disease. N Engl J Med 320:1446–1452.

Schinder AF, Olson EC, Spitzer NC, Montal M (1996) Mitochondrial dysfunction is a primary event in glutamate neurotoxicity. J Neurosci 16:6125–6133.

Sinet PM (1982) Metabolism of oxygen derivatives in Down's syndrome. Ann NY Acad Sci 396:83–94.

Stabel-Burow J, Kleu A, Schuchmann S, Heinemann U (1997) Glutathione levels and nerve cell loss in hippocampal cultures from trisomy 16 mouse: a model of Down syndrome. Brain Res 765:313–318.

Starkov AA, Markova OV, Mokhova EN, Arrigoni-Martelli E, Bobyleva VA (1994) Fatty acid-induced Ca^{2+}-dependent uncoupling and activation of external pathway of NADH oxidation are coupled to cyclosporin A-sensitive mitochondrial permeability transition. Biochem Mol Biol Int 32:1147–1155.

Takeyama N, Matsuo N, Tanaka T (1993) Oxidative damage to mitochondria is mediated by the Ca^{2+}-dependent inner membrane permeability transition. Biochem J 294:719–725.

Tymianski M, Wallace MC, Spigelman I, Uno M, Carlen PL, Tator CH, Charlton MP (1993) Cell-permeant Ca^{2+} chelators reduce early excitotoxic and ischemic neuronal injury in vitro and in vivo. Neuron 11:221–235.

Waring P, Beaver J (1996) Cyclosporin A rescues thymocytes from apoptosis induced by very low concentrations of thapsigargin: effects on mitochondrial function. Exp Cell Res 227:264–276.

Weis M, Kass GEN, Orrenius S (1994) Further characterization of the events involved in mitochondrial Ca^{2+} release and pore formation by prooxidants. Biochem Pharmacol 47:2147–2156.

White RJ, Reynolds IJ (1995) Mitochondria and Na^{+}/Ca^{2+} exchanger buffer glutamate-induced calcium loads in cultured cortical neurons. J Neurosci 15:1318–1328.

White RJ, Reynolds IJ (1996) Mitochondrial depolarization in glutamate-stimulated neurons: an early signal specific to excitotoxin exposure. J Neurosci 16:5688–5697.

Yim MB, Chock PB, Stadtman ER (1993) Enzyme function of copper, zinc superoxide dismutase as a free radical generator. J Biol Chem 268:4099–4105.

Zamzami N, Marchetti P, Castedo M, Hirsch T, Susin SA, Masse B, Kroemer G (1996) Inhibitor of permeability transition interfere with the disruption of the mitochondrial transmembrane potential during apoptosis. FEBS Lett 384:53–57.

Zazueta C, Reyes-Vivas H, Corona N, Bravo C, Chávez E (1994) On the role of ADP to increase the inhibitory effect of cyclosporin on mitochondrial membrane permeability transition. Biochem Mol Biol Int 33:385–392.